ATMOSPHERELESS COSMIC BODIES (MOON, MARTIAN SATELLITES, COMETS) AND DUSTY PLASMA EFFECTS

S.I. Popel, A.P. Golub', L.M. Zelenyi

Space Research Institute RAS, Moscow, Russia

Contents

- Future Lunar Missions
- Dusty Plasma System in the Vicinity of the Moon
- Lunar Terminator
- Effects of Micrometeoroids
- Dusty plasmas at Phobos and Deimos
- Dusty plasmas at comets
- Interaction of Solar wind with comet
- Conclusions

Future Lunar Missions

A renaissance is currently being observed in investigations of the Moon, which are planned in the PR of China, United States, India, and European Union. The Luna 25 and Luna 27 missions are being prepared in Russia.

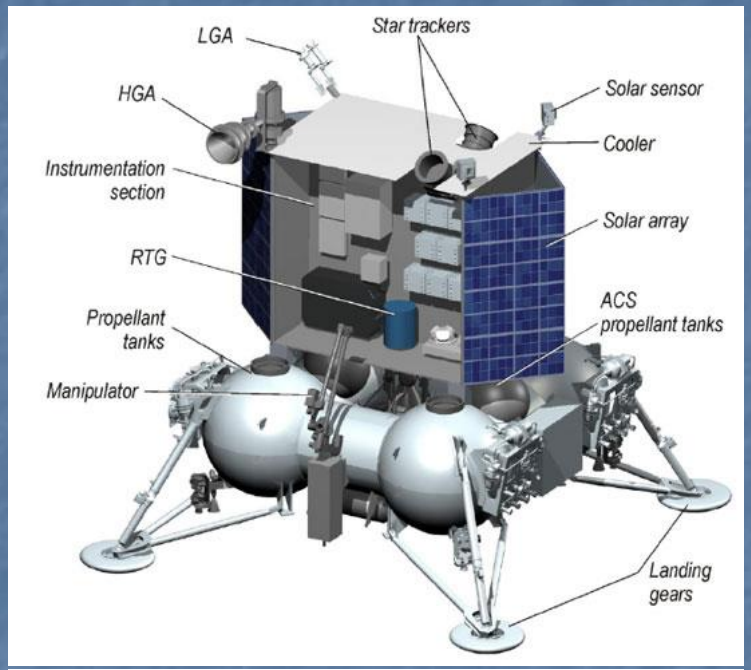

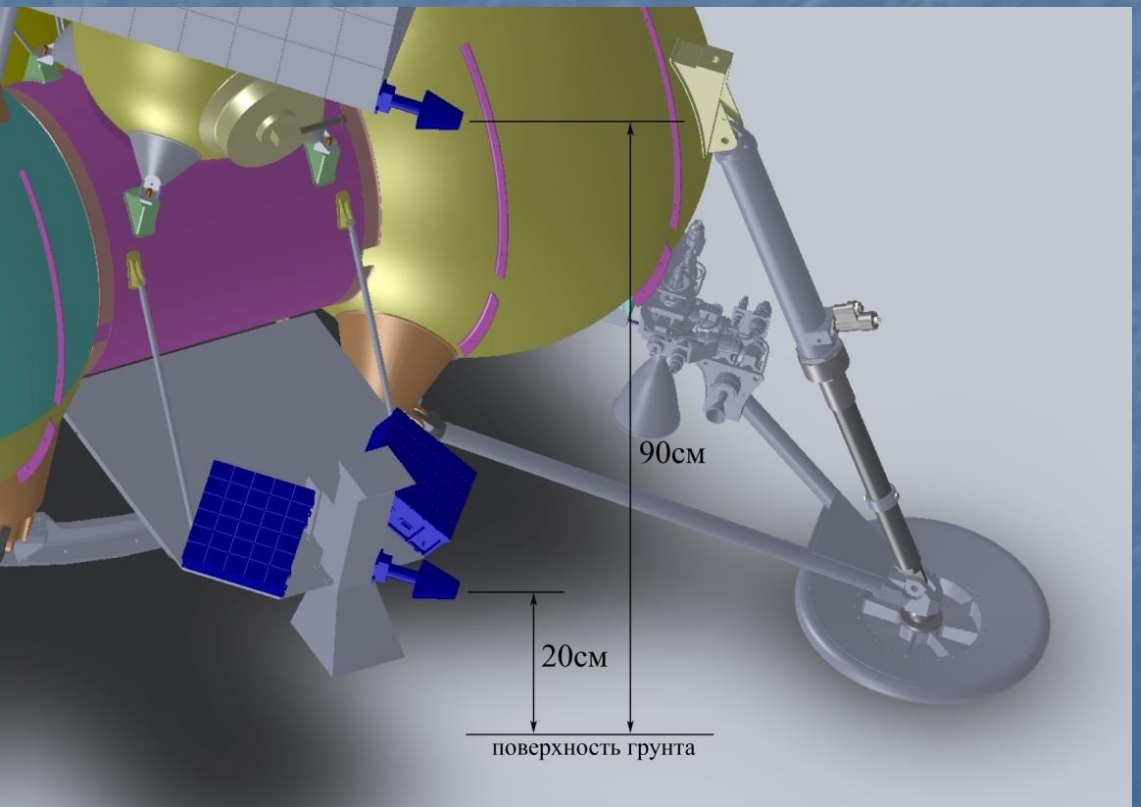

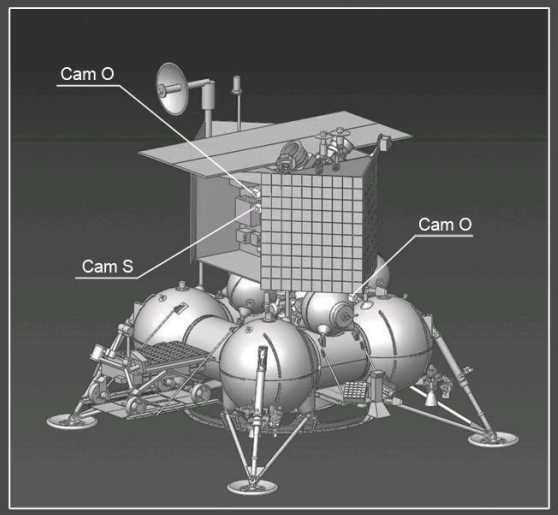

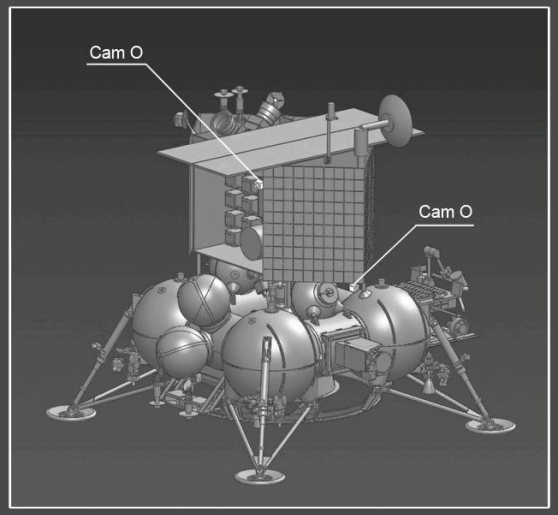

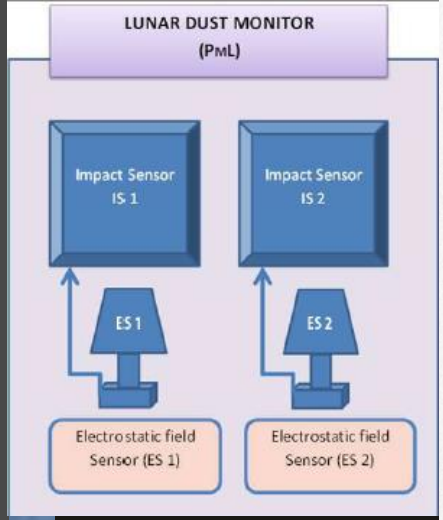

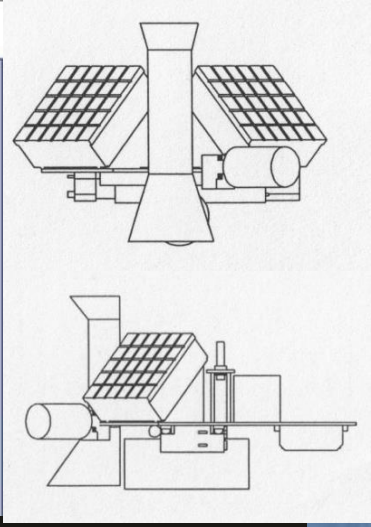

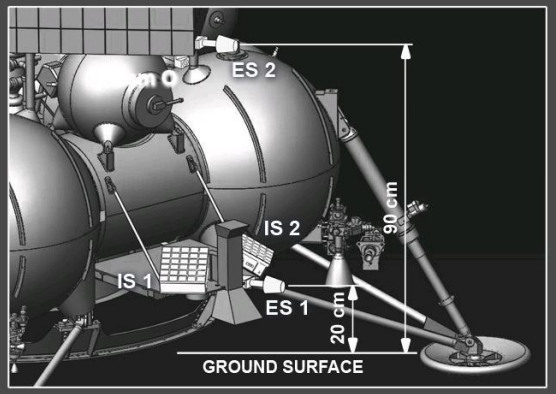

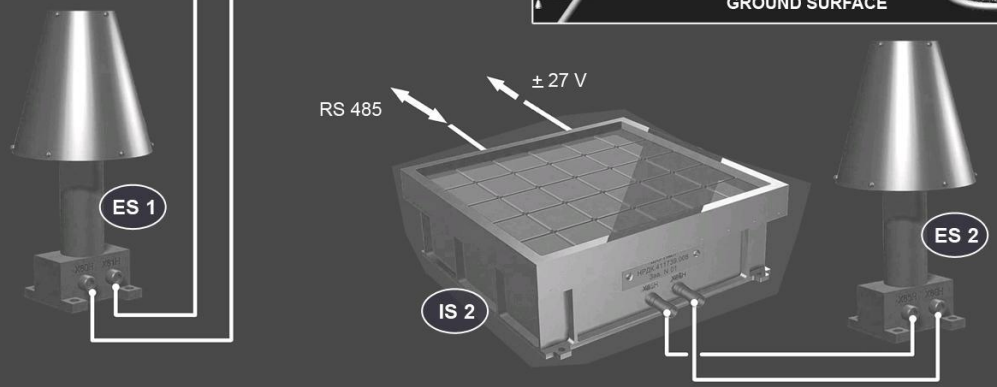

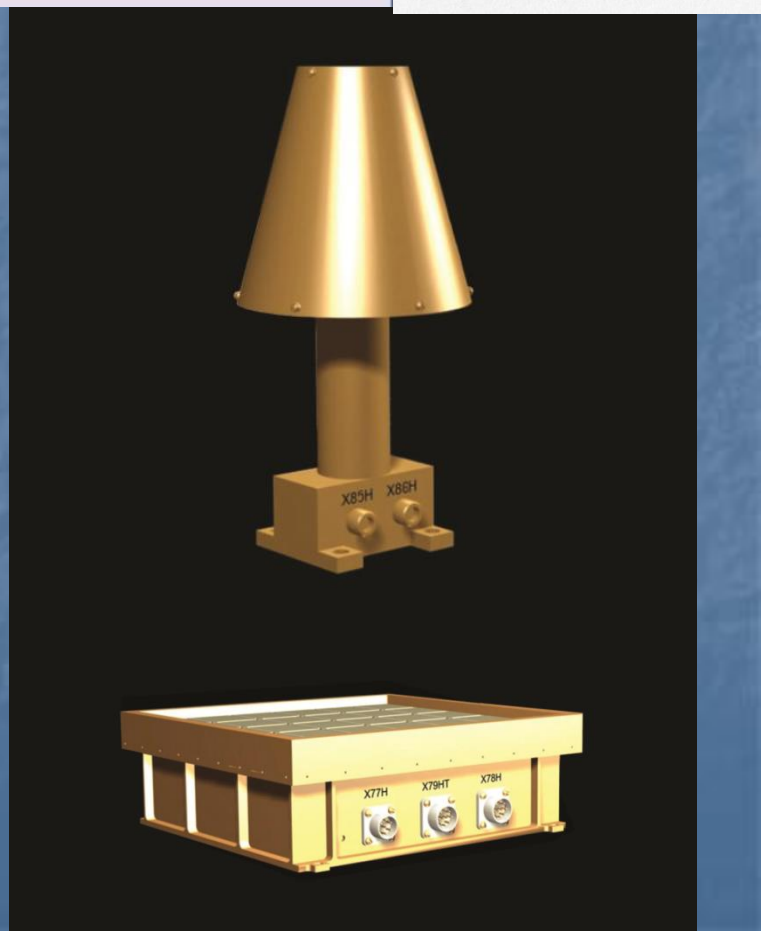

IS - impuct sensor ; **ES** - electrostatic sensor ; **Cam O** - onerview camera ; **Cam S** - stereocamera ; RS -

Ground Experiment for Test Method of Lunar Dust Monitor

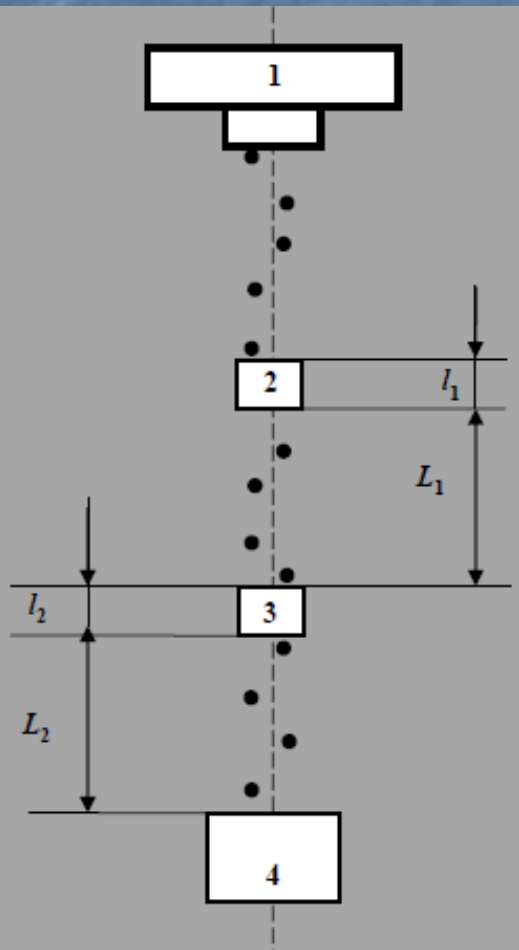

On sketch:

1 - injector dust particles;

2 - first induction sensor;

3 - second induction sensor;

4 - piezoceramic sensor.

l_1 = 71 mm l_2 = 64 mm

L_1 = 293 mm L_2 = 572 mm

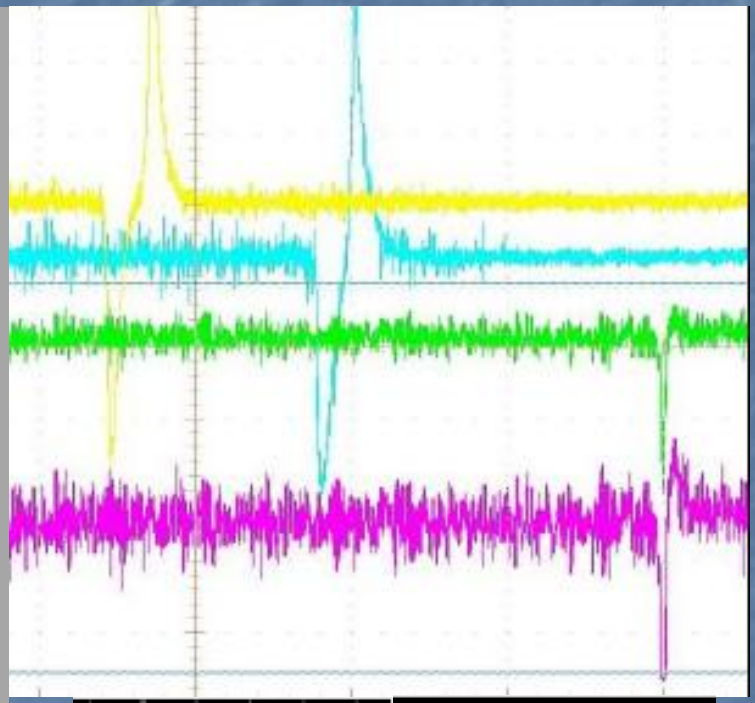

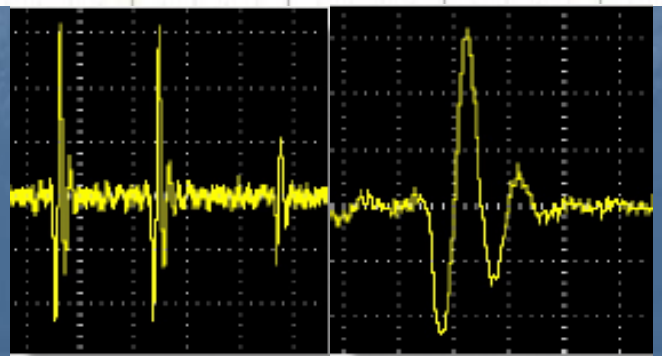

Observations of Lunar Dust

- From the Apollo era of exploration it was discovered that sunlight was scattered at the terminators giving rise to "horizon glow" and "streamers" above the lunar surface (Rennilson and Criswell, *Moon* **10**, 121 (1974)). Subsequent investigations have shown that the sunlight was most likely scattered by electrostatically charged dust grains originating from the surface (*e.g.*, Zook and McCoy, *GRL* **18**, 21171 (1991)). The Surveyor landers observed ≈5 μm grains levitating ~10 cm above the surface. During the Apollo missions 0.1 μm-scale dust in the lunar exosphere was observed up to ~100 km altitude.

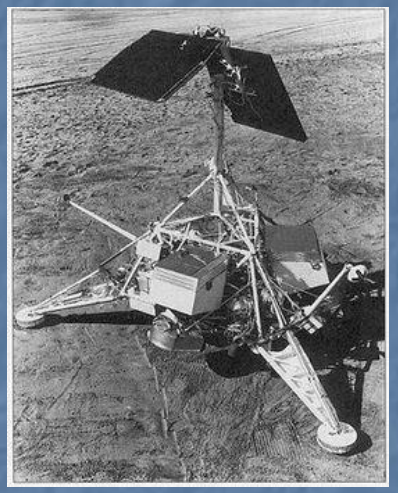

Surveyor -7

Lunar Prospector

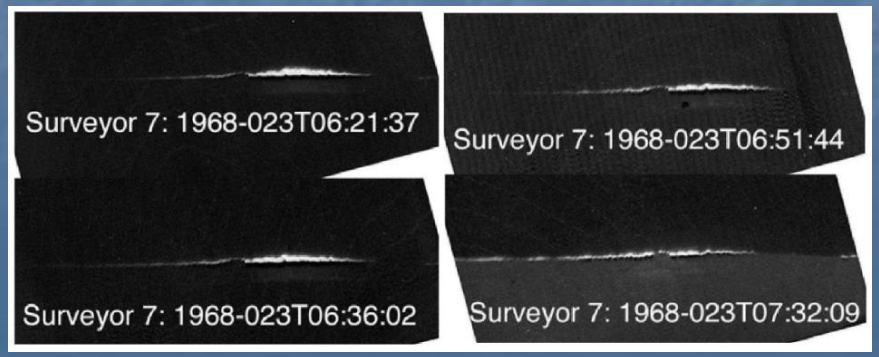

Apollo-17

Dust on the Moon

	«Apollo-11»	«Luna-20»	«Apollo-15»	«Apollo-14»	«Apollo-12»
SiO_2	40.5	42.4	44.1	50.0	61.0
Al_2O_3	9.7	20.2	35.5	20.0	12.0
FeO	19.0	6.4	0.2	7.7	10.0
TiO_2	11.4	0.4	-	1.3	1.2
CaO	9.6	18.6	19.7	11.0	6.3
MgO	8.0	12.2	0.1	8.0	6.0
Na_2O	0.53	0.4	0.34	0.63	0.69
K_2O	0.16	0.52	-	0.53	2.0

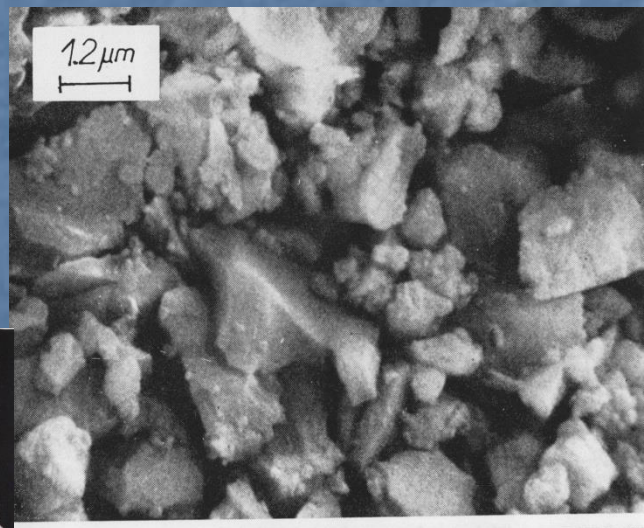

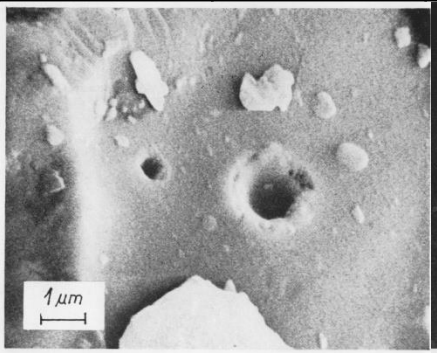

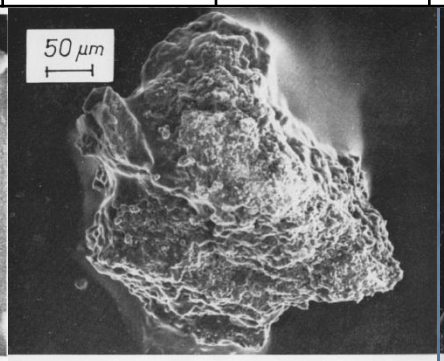

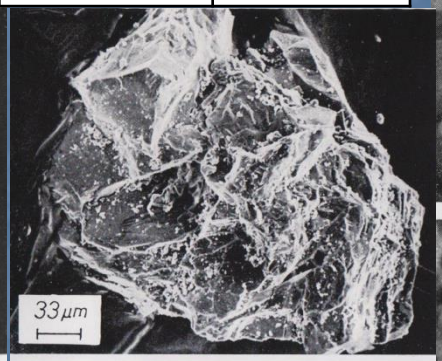

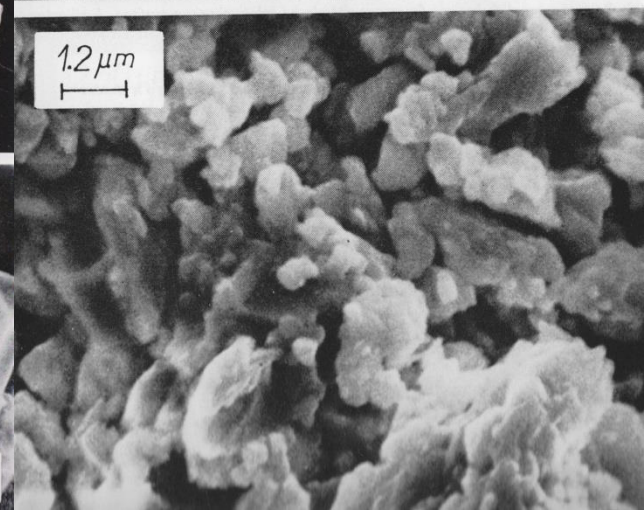

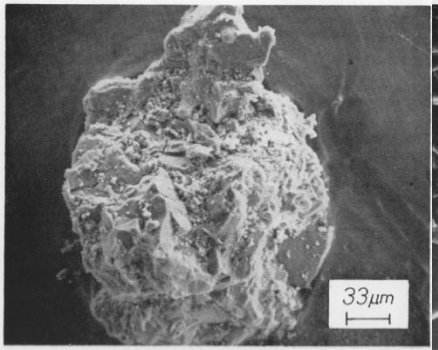

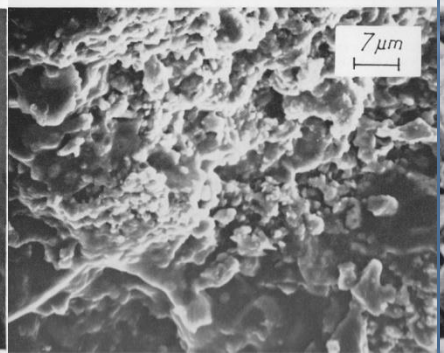

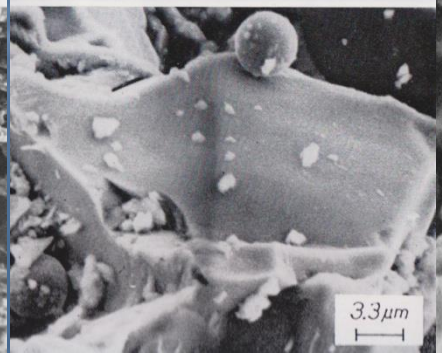

Dusty Plasma System in the Vicinity of the Moon

- Since the Moon is in the solar wind plasma flow for most of its orbit, lunar dust constitutes a part of a dusty plasma system. This takes also place for the situation when the Moon is not in the solar wind. For about one-quarter of its orbit, the Moon is either in the tenuous plasma of the Earth's magnetospheric tail lobes, or the turbulent and energetic plasmas encountered in the magnetosheath and the plasma sheet. At the orbit of the Moon, the plasma conditions in the magnetosheath are not significantly different from those in the solar wind. However, inside the magnetosphere, the plasma environments are typically much more tenuous and significantly hotter than in the solar wind. The plasma sheet is much hotter than the tail lobes. This is an important factor for dust grain charging in the dusty plasma system in the vicinity of the Moon.

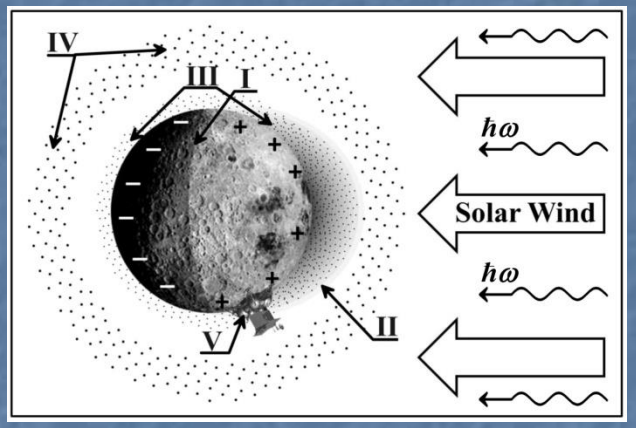

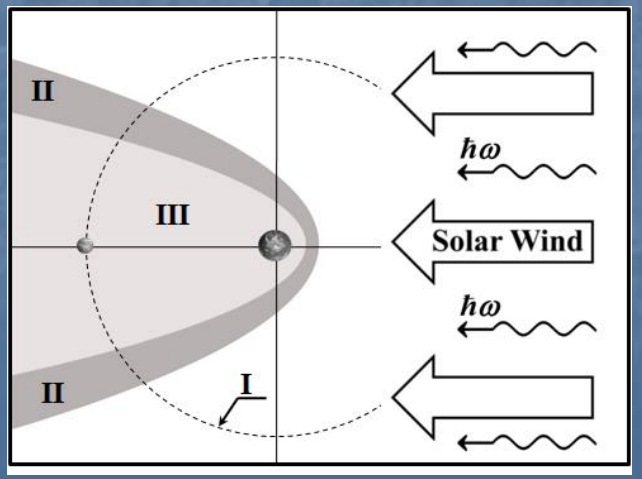

Research on the Lunar Dusty Plasma Effects

T. Stubbs et al. *Adv. Space Res.* **37,** 59 (2006).

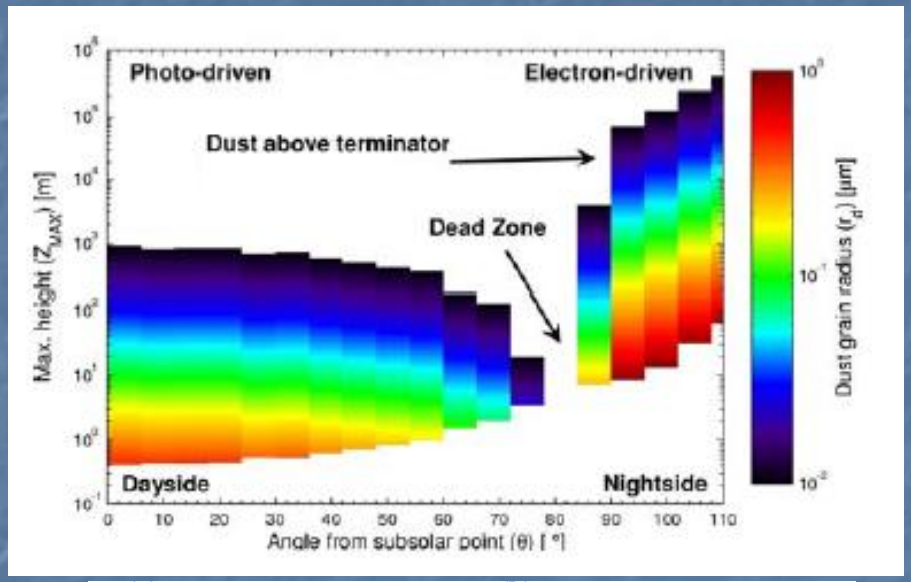

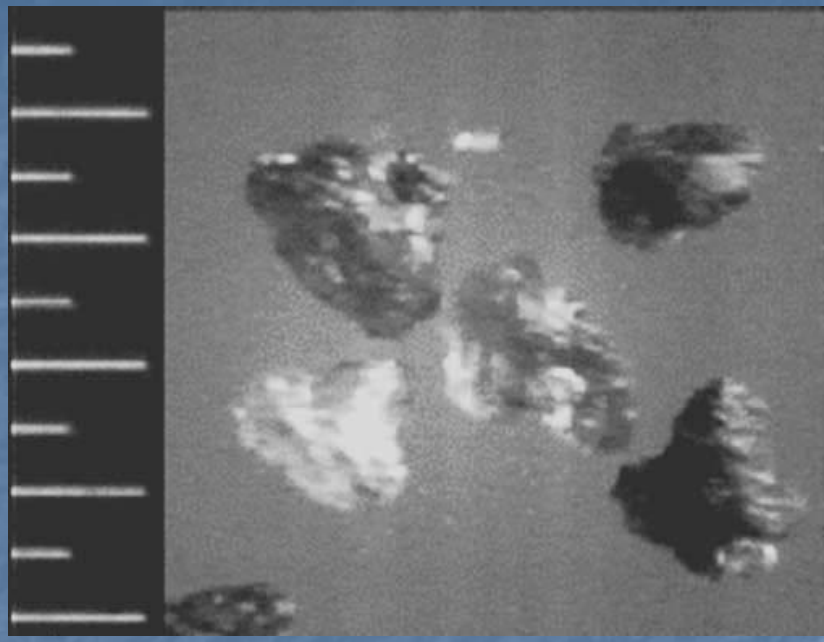

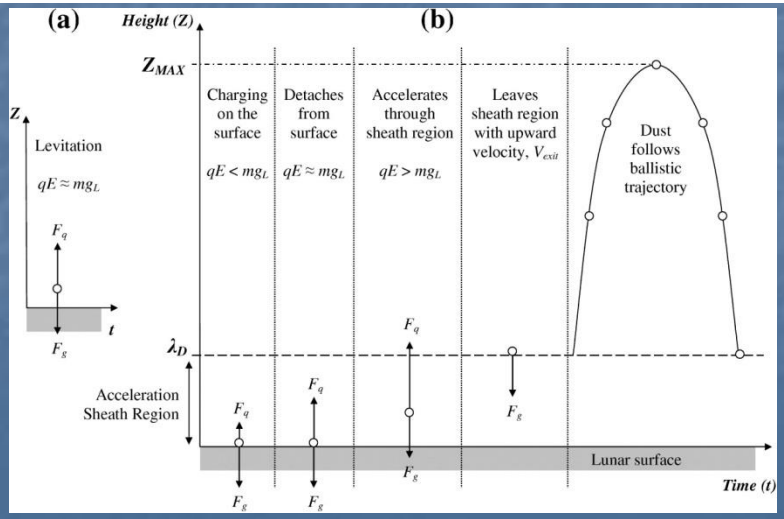

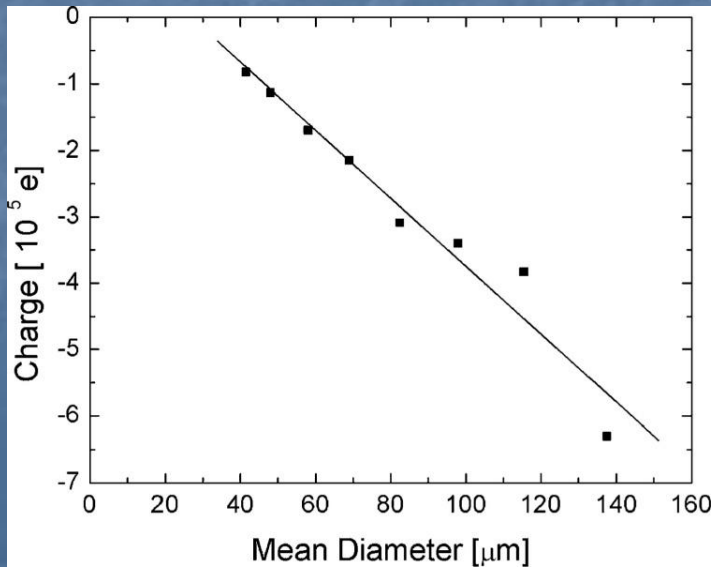

Sternovsky et al. *JGR* **107**, 5105 (2002) =>

New Data from LRO

- Recent detections (Mitrofanov et al., *Science* **330**, 483 (2010)) of neutron fluxes passing through regions of the surface of the Moon in the Southern Hemisphere of the Moon on the Lunar Reconnaissance Orbiter show the existence of hydrogen-enriched regions in the surface layer of the Moon at lunar latitudes exceeding 70°. The investigation possibly indicates the existence of ice in surface regions of the Moon, and the existence of surface regions of hydrogen is possibly due to electrons and protons of the solar wind, which collide with the Moon and are absorbed by its surface, where they form neutral hydrogen atoms. This hydrogen can rise on the surface of the Moon in the form of atomic or molecular hydrogen or water vapor. In this case, the sensitivity of the hydrogen-enriched regions of the surface of the Moon to photoemission is much higher than that of surrounding regions; this finally affects the charging of dust particles and their dynamics.

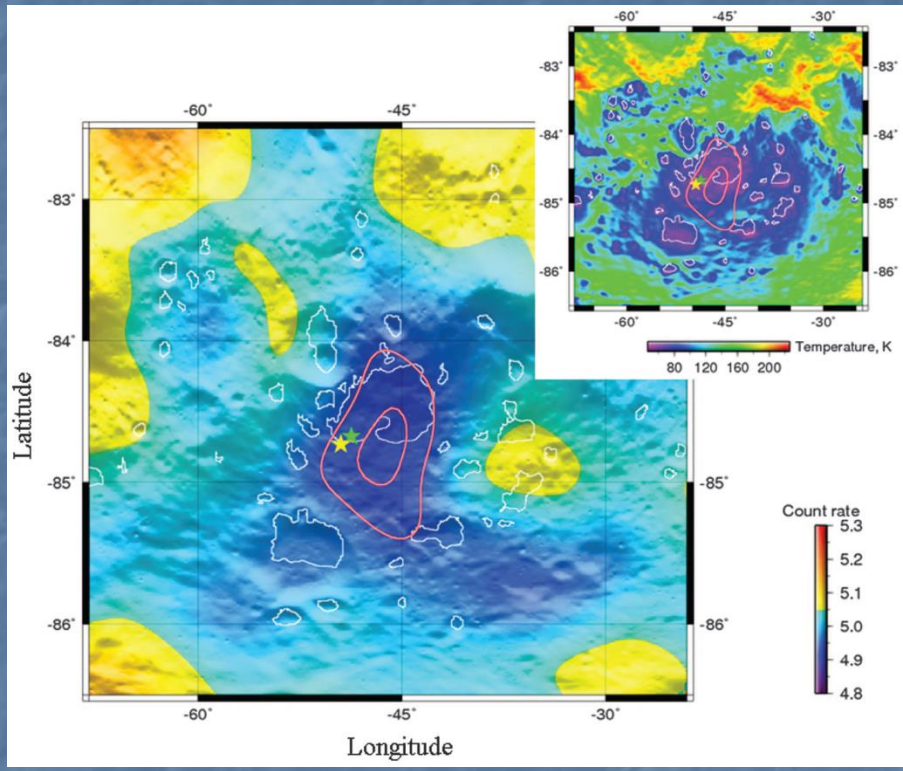

Hydrogen Mapping of the Lunar South Pole Using the LRO Neutron Detector Experiment LEND

Self-Consistent Model

- The effects of **photoelectrons** from both the lunar surface and dust particle surfaces, electrons and ions of the solar wind, and solar radiation are taken into account.
- The set of equations consists of the **steady state kinetic equation for the distribution function of electrons** and the **Poisson equation** for the electrostatic potential with the corresponding boundary conditions characterizing the behavior of the potential near the surface of the Moon and at an infinite distance from it.
- The number of photoelectrons near the surface of the Moon that are knocked out from the surface of the by photons is calculated using the data on the solar radiation spectrum and the quantum photoemission yield.
- The resulting velocity distribution of photoelectrons near the surface of the Moon is approximated by a Maxwellian distribution (for two photoemission workfunctions *4 eV and 6 eV).*
- Dust motion in the electrostatic electric field and dust particle charging are taken into account.

Spectrum of Solar Radiation

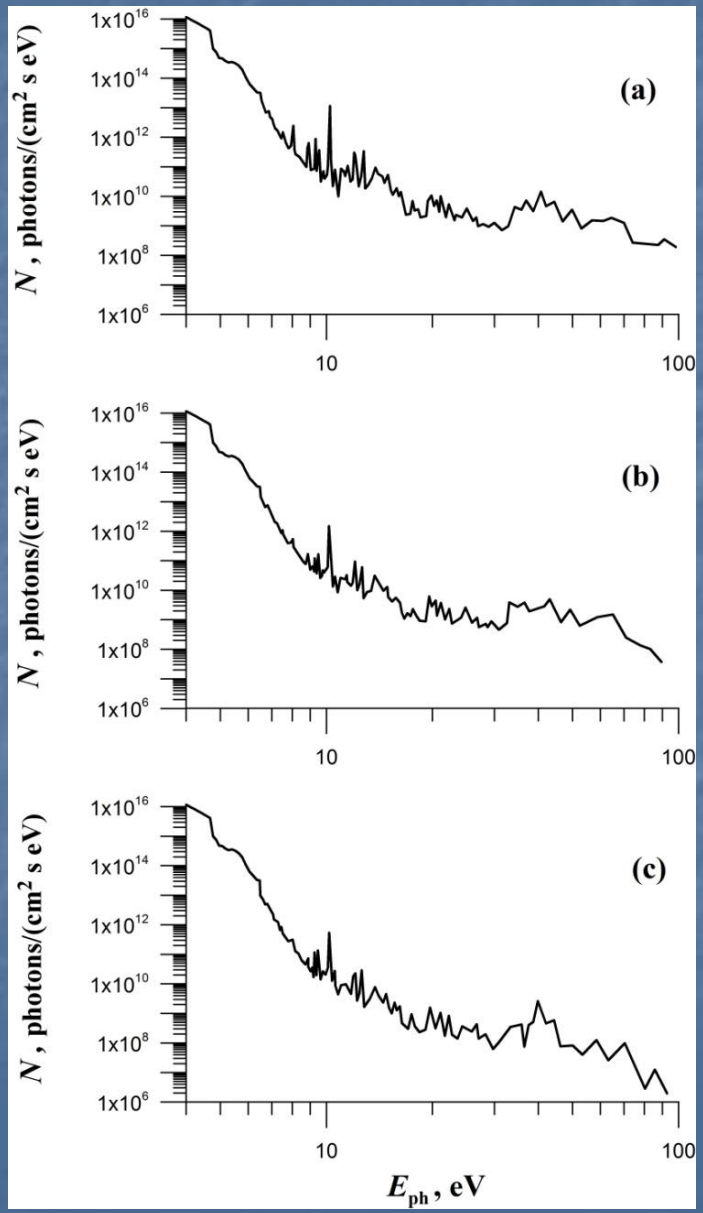

- Electrons over the lunar dayside appear due to the photoemission from the lunar surface as well as from the surfaces of dust particles levitating over the Moon, while the photoelectron emission is due to the solar vacuum ultraviolet (VUV) radiation. During the 11-year solar cycle the amount of radiated VUV energy changes significantly, that results in a significant variation in the photoelectron current. Here, we present the results of our calculations for three different solar activity conditions. These are the solar minimum, solar maximum,an X28 class solar flare event.

Photoelectrons near the Lunar Surface

$$\Phi_e(E_e)dE_e = 2\cos\theta\sqrt{\frac{2m_e}{E_e}}\int_{E_e+W}^{\infty} Y(E_{ph})F_{ph}d\rho dE_{ph},$$

$$d\rho = \frac{6(E_m - E_e)}{E_m^3}E_e dE_e, \qquad 0 \le E_e \le E_m = E_{ph} - W$$

$$N_0 = \int_0^{\infty} \Phi_e(E_e)dE_e,$$

$$T_e = \frac{2}{3}\langle E_e\rangle \equiv \frac{2}{3N_0}\int_0^{\infty} E_e\Phi_e(E_e)dE_e.$$

<u>Hydrogen</u>

$Y = Y(\varepsilon_\Phi)$ = (Kolesnikov & Manuilov)

$= 0.1125\varepsilon_\phi - 0.4$ for $4 \le \varepsilon_\phi \le 8$ eV

$= 0.5$ for $8 < \varepsilon_\phi \le 25$ eV.

W_H=4 eV

<u>Regolith</u>:

$Y = Y(\varepsilon_\Phi)$ = (Walbridge)

$= 0.02 + 0.06 \times (\varepsilon_\phi - 6)$ for $6 \le \varepsilon_\phi \le 9$ eV

$= 0.2$ for $\varepsilon_\phi > 9$ eV.

W_R=6 eV

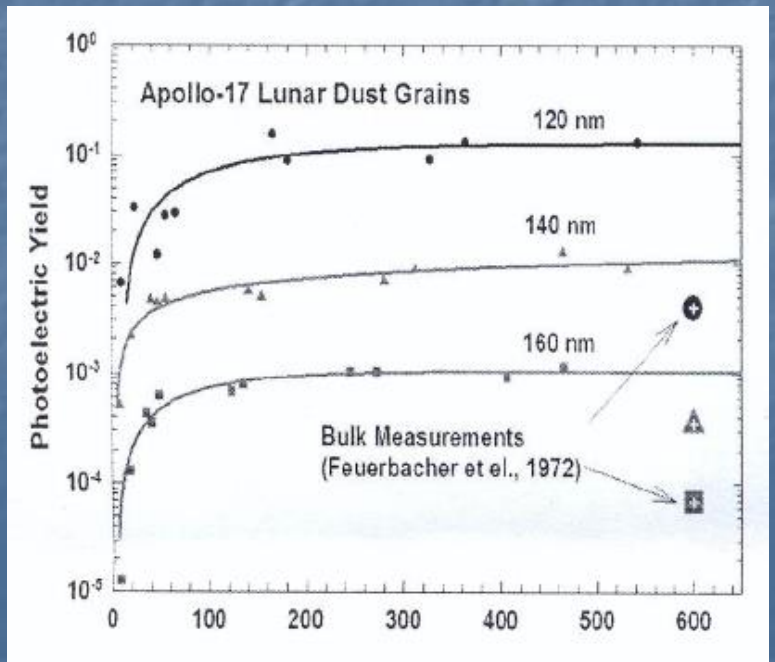

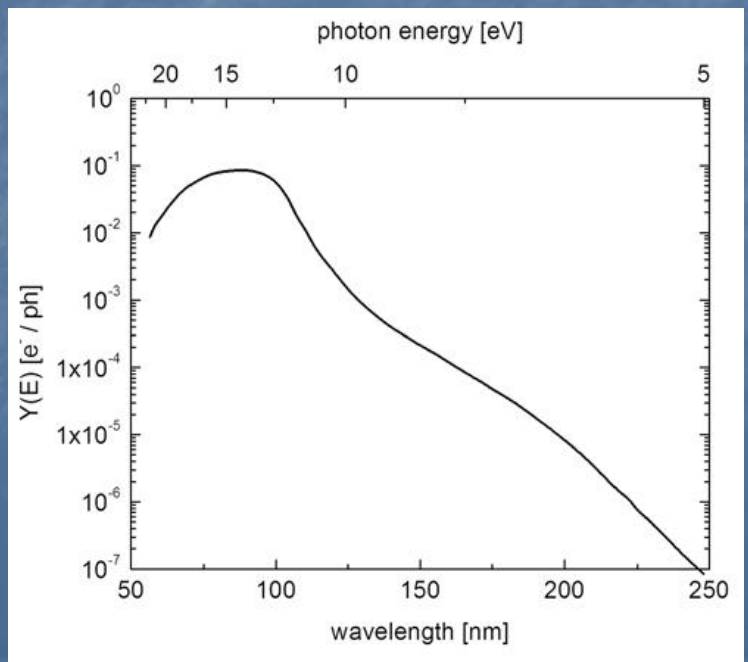

Photoelectron Distribution near the Lunar Surface

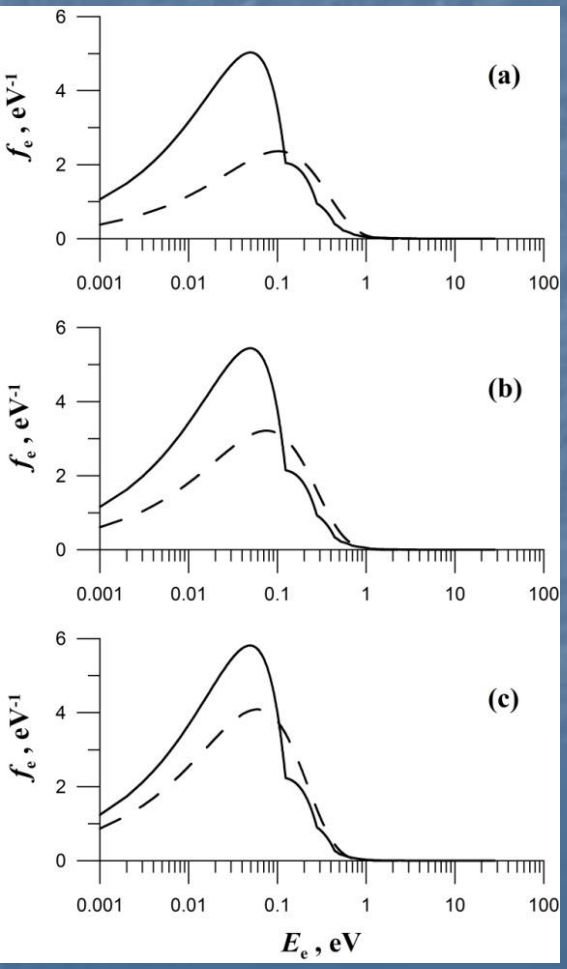

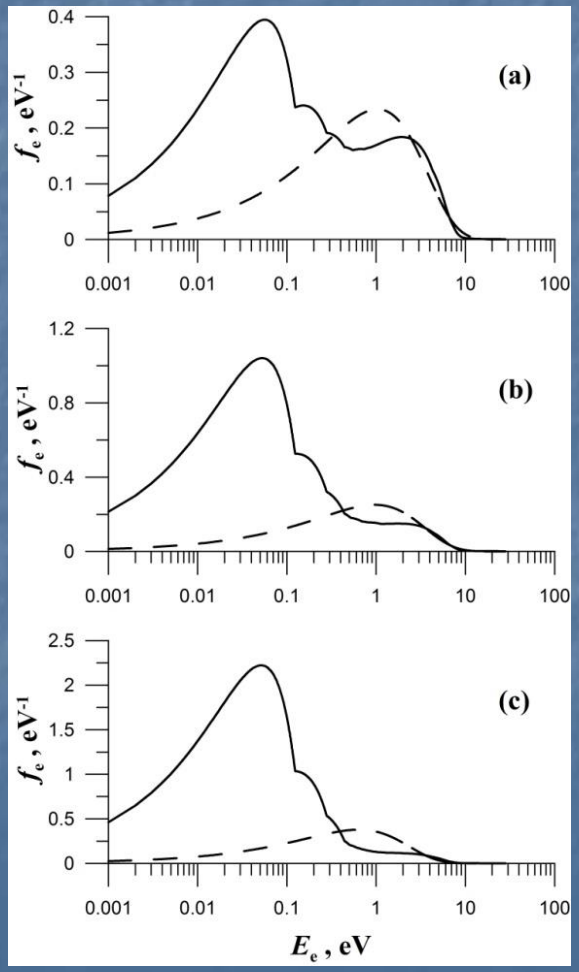

	I	II	III
N_{01}, cm^{-3}	$2.2 \cdot 10^5$	$2.1 \cdot 10^5$	$1.9 \cdot 10^5$
T_{e1}, eV	0.2	0.1	0.1

	I	II	III
N_{02}, cm^{-3}	$8.6 \cdot 10^2$	$2.9 \cdot 10^2$	$1.3 \cdot 10^2$
T_{e2}, eV	2.1	1.9	1.3

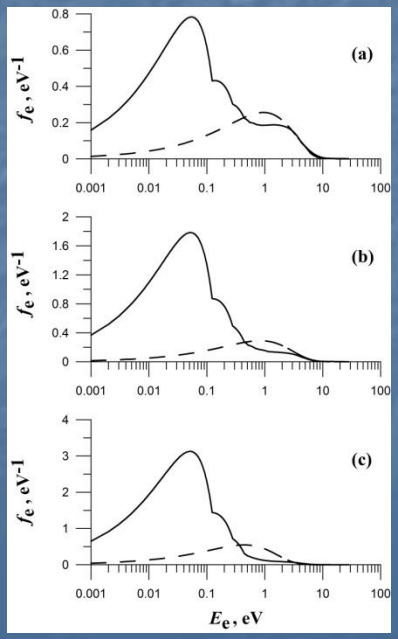

Yield Measurement on the Lunar Surface (I)

- The main factor influencing the photoelectron number density and the photoelectron temperature near the lunar surface is the quantum photoemission yield. At present, there is no adequate research concerning the quantum photoemission yield of the lunar regolith. The significance of this parameter is great because, in particular, it influences the structure of the dusty plasma system over the Moon and determines it to a great extent. In this connection the future in-situ measurements of the lunar surface quantum photoemission yield (and work functions) are of great importance, and the corresponding investigations should be planned for the future lunar missions.

Yield Measurement on the Lunar Surface (II)

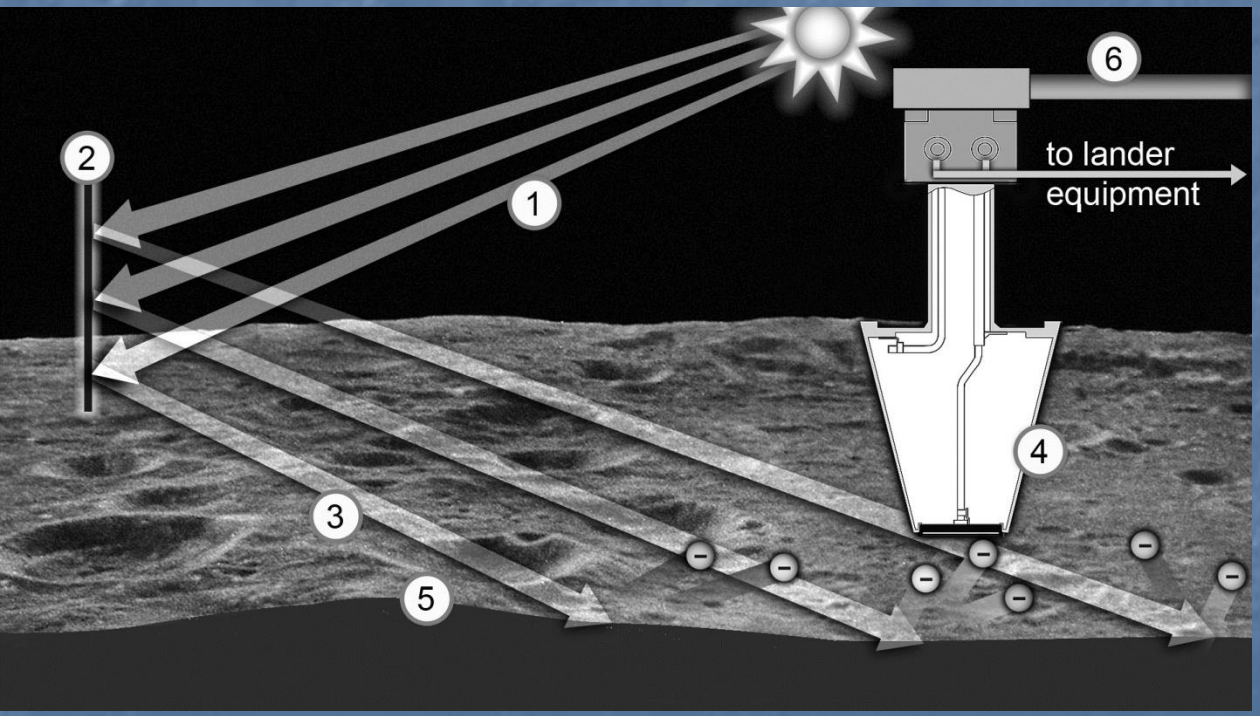

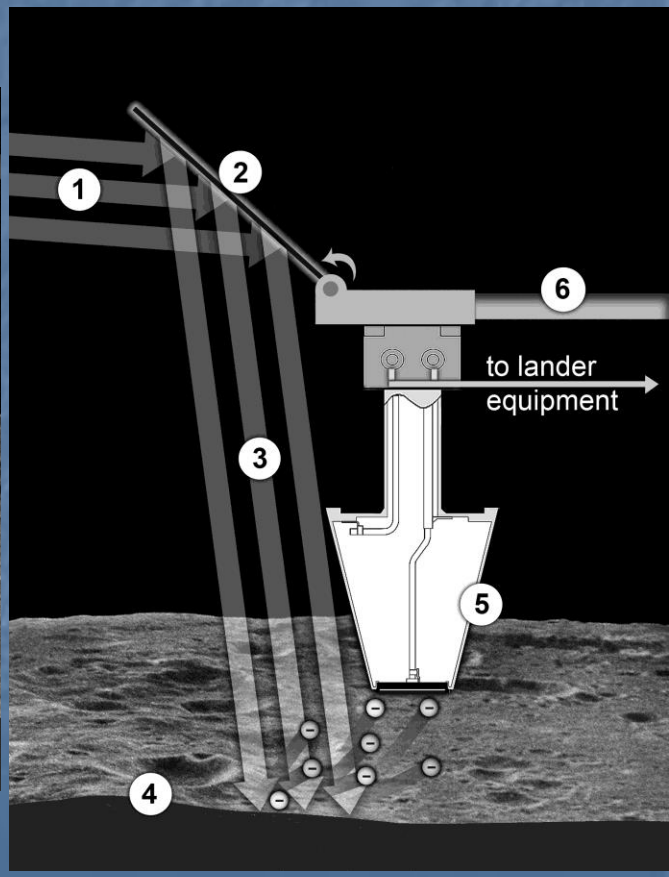

Electron Distributions over the Moon

$$n_{e,\mathrm{ph}} \approx N_0 \frac{\cos\theta}{[1+\sqrt{\cos\theta/2}(h/\lambda_D)]^2} + N_e (h/h_1)^{\alpha}$$

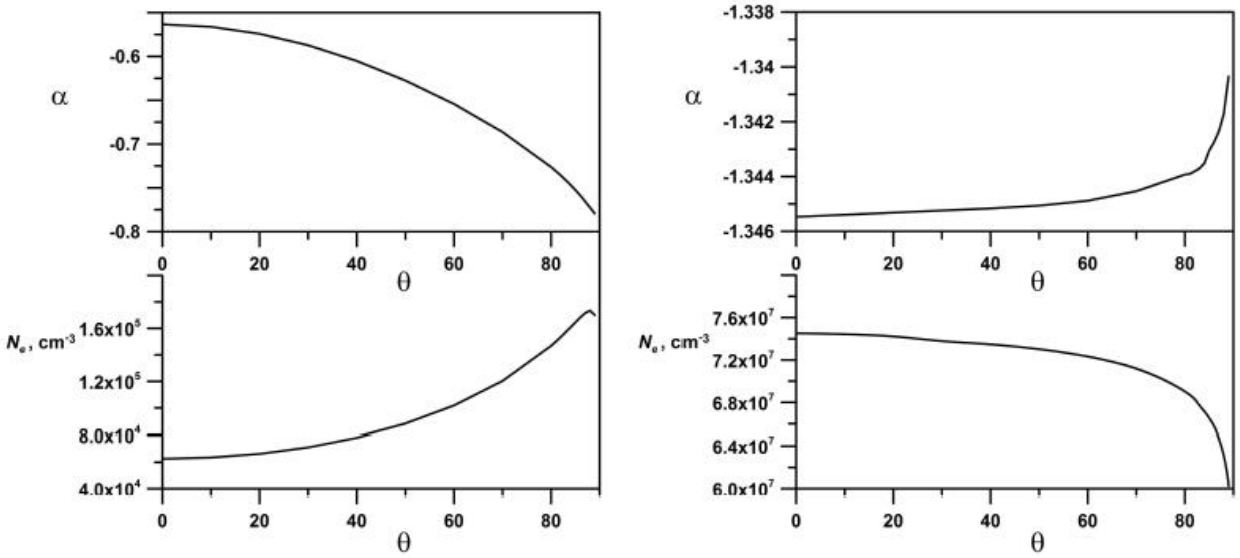

Figure 1: The constants α and N_e *vs* θ for regolith regions (left panel) and hydrogen-enriched regions (right panel) of the surface of the Moon

Parameters of Dust

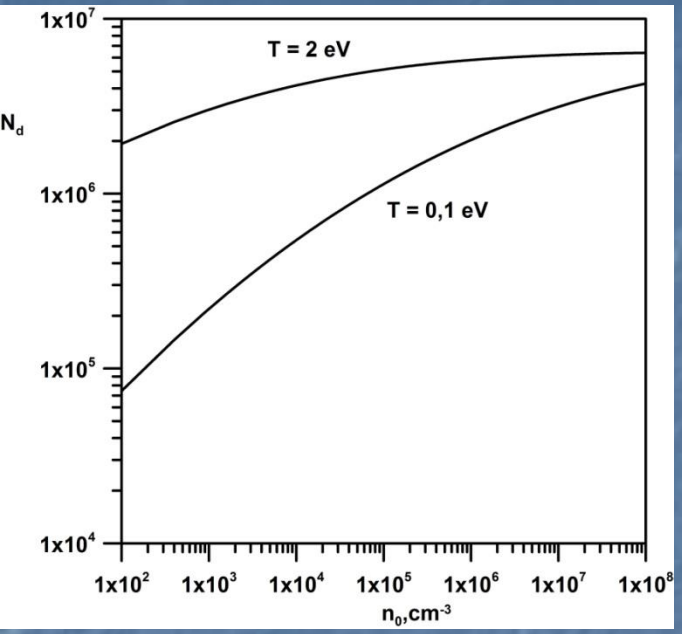

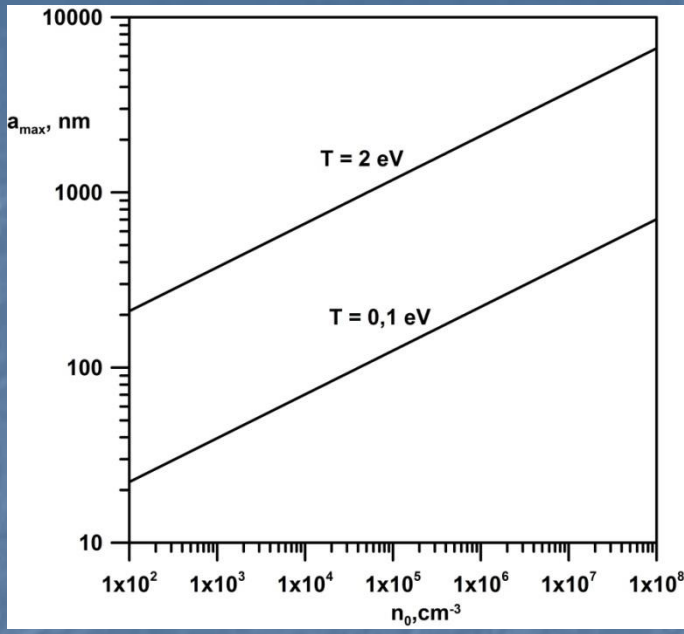

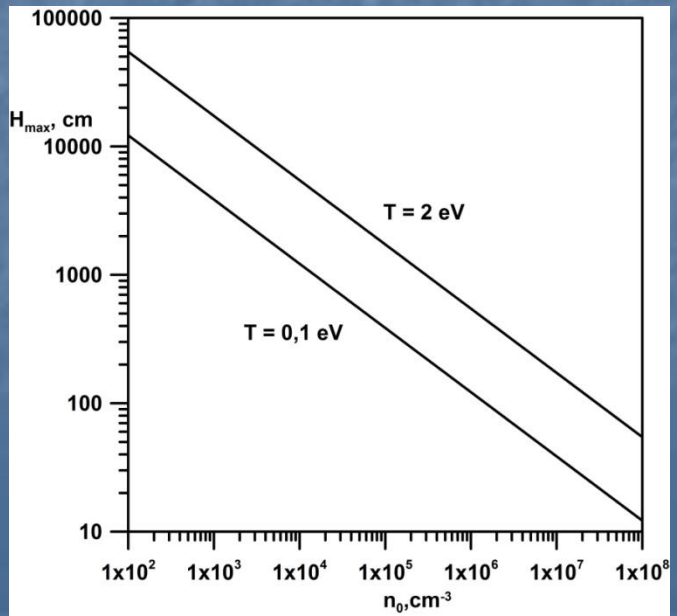

Size Distribution of Dust Particles over the Moon

The probability of the presence of a particle at a certain height (which is inversely proportional to the time of presence of a particle at this height) is calculated. This probability is multiplied by a normalization factor, which is calculated to ensure an adequate description of the size distribution of surface lunar dust. To determine the normalization factor, we used the data from Colwell et al., Rev. Geophys. **45,** RG2006 (2007) that made it possible to plot the distribution of dust particles of the surface of the Moon in the size range from 20 to 500 μm. This distribution is in good agreement with the Kolmogorov distribution, which is the size distribution of particles in the case of multiple crushing. This fact is in agreement with the one that the surface of the Moon is regolith evolving because of multiple crushing under meteorite impacts. The Kolmogorov distribution for the case of multiple crushing is valid at least for particles with sizes 100 nm (Adushkin et al, *Dokl. Earth Sci.* **415**, 820 (2007)).

$$d\Phi(L) = \frac{dm}{M} = \frac{1}{\sqrt{2\pi}\sigma_{\ln L} L} e^{-\frac{(\ln L - \ln L_{50})^2}{2\sigma_{\ln L}^2}} dL$$

σ_L = 1.29 is the parameter of the Kolmogorov distribution; and Ln(L_50) = ln61.56 ≈ 4.12 is the median of the Kolmogorov distribution

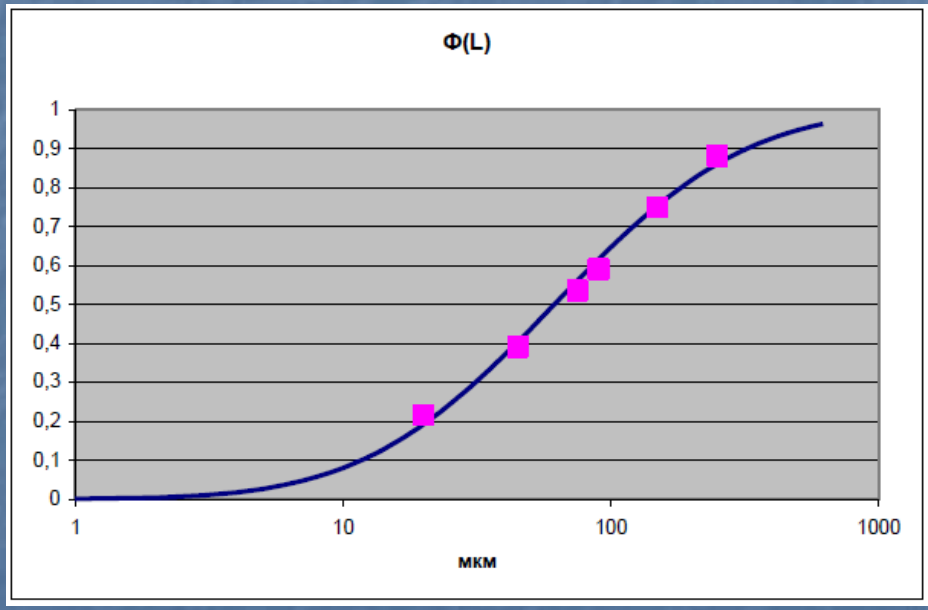

Grain size, μm						
	250-500	150-250	90-150	75-90	45-75	20-45
Weight per cent	11.91	13.13	15.99	5.48	14.45	17.37

Dust Distributions for Lunar Regolith Regions

$$dN_d \approx \frac{A}{\sqrt{2\pi}\sigma a^4}\exp\left\{-\frac{[\ln(a)-\mathrm{Ln}]^2}{2\sigma^2}\right\} \times \frac{da}{\tau_{\max}\sqrt{4Z_d(h,\theta)\left(\frac{T_{e,\mathrm{ph}}}{m_d}\right)\ln\left[1+\sqrt{\cos\frac{\theta}{2}}\left(\frac{h}{\lambda_D}\right)\right]-2g_M h}}, \quad (8)$$

Here,

$$\tau_{\max} = \int_0^{H_{\max}} \frac{dh}{\sqrt{4Z_d(h,\theta)\left(\frac{T_{e,\mathrm{ph}}}{m_d}\right)\ln\left[1+\sqrt{\cos\frac{\theta}{2}}\left(\frac{h}{\lambda_D}\right)\right]-2g_M h}}, \quad (9)$$

where *Hmax* is the maximum rise height of the dust particle with the size *a* (measured in microns); *A* ≈ *8.48* × 10^{–4} cm has the meaning of the effective depth of the dust layer that can be separated from the surface.

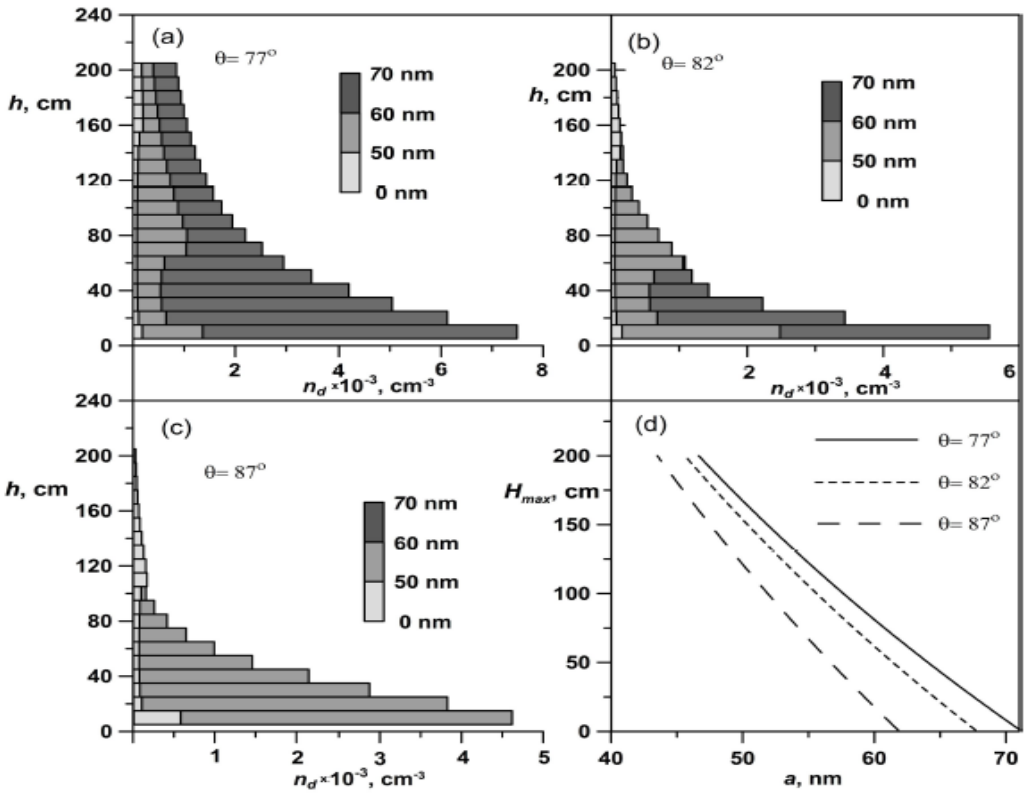

Figure 2: Distributions of dust particles over the surface of the Moon for $\theta = 77^o$ (a), 82^o (b), and 87^o (c) as well as dependencies of maximum possible rise heights H_{max} (d) of dust particles on their sizes a under the conditions corresponding to the lunar regolith regions

Dust distributions for Hydrogen-Enriched Regions (θ = 77°, 82°, and 87°)

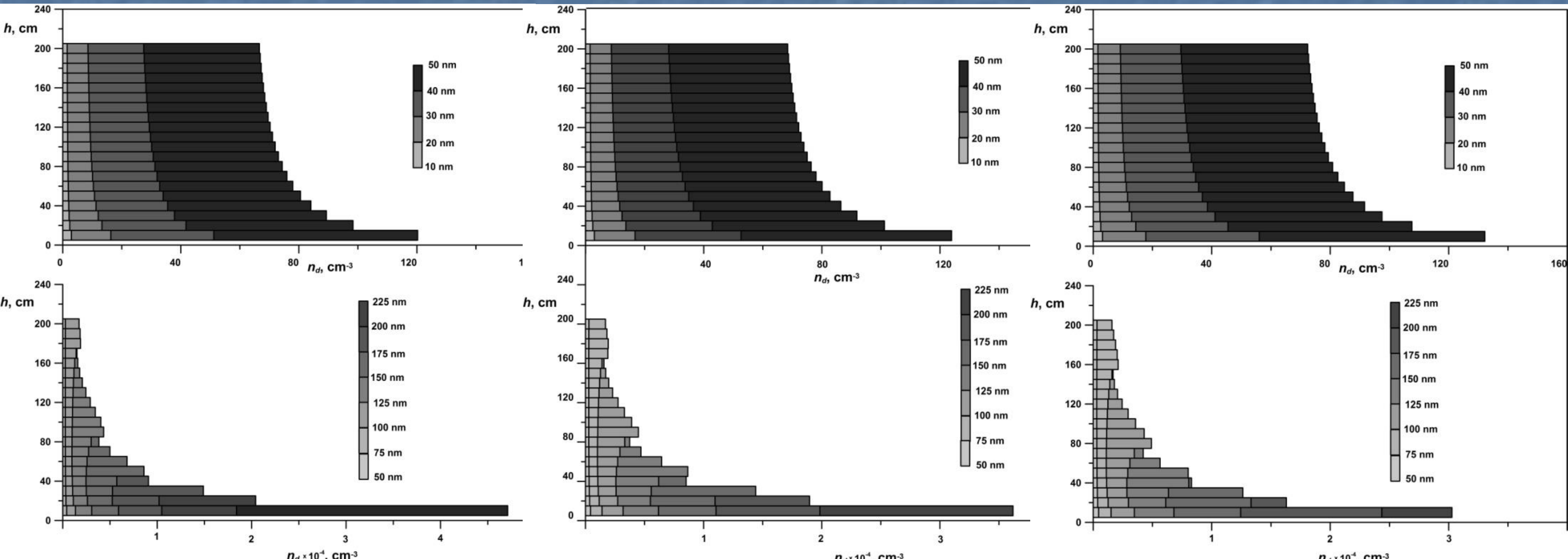

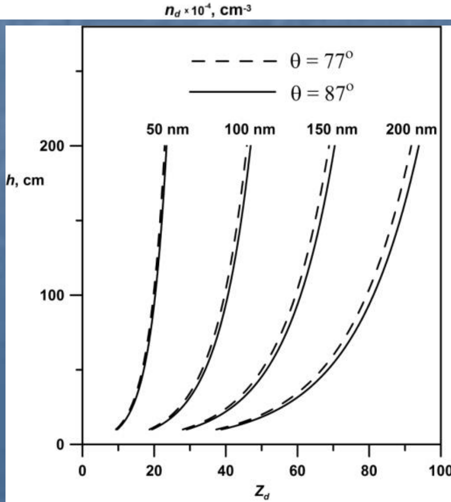

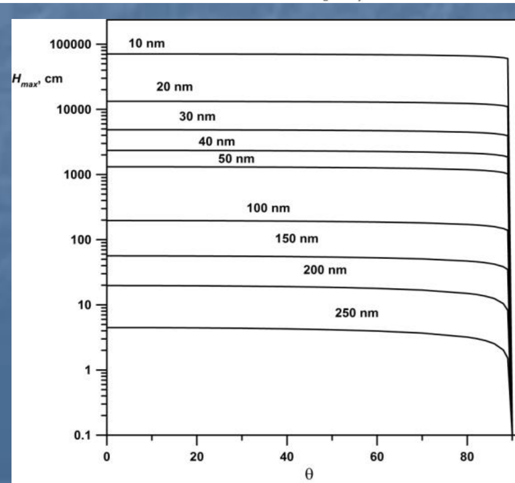

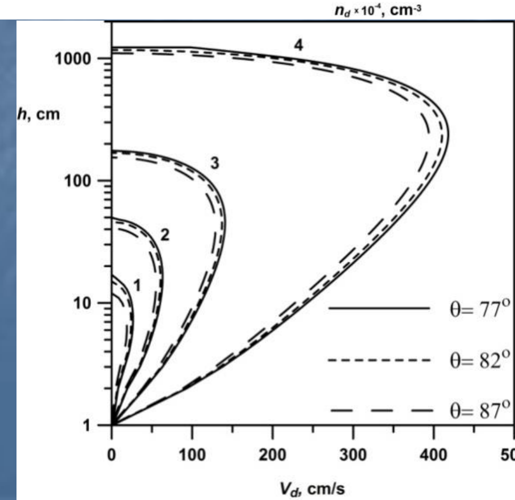

Electric Fields

80°

h, cm	E(h) CGSE	E(h) SI
0	0,011838314	355,1494
0,01	0,010053132	301,5939
0,1	0,004264911	127,9473
1	0,000631125	18,93376
10	6,62933E-05	1,9888
20	3,32397E-05	0,997192
30	2,21806E-05	0,665418
40	1,66432E-05	0,499297
50	1,33183E-05	0,39955
60	1,11007E-05	0,333021
70	9,51615E-06	0,285485
80	8,32747E-06	0,249824
90	7,40278E-06	0,222083
100	6,66291E-06	0,199887
110	6,0575E-06	0,181725
120	5,55295E-06	0,166588
130	5,12598E-06	0,15378
140	4,75999E-06	0,1428
150	4,44278E-06	0,133283
160	4,1652E-06	0,124956
170	3,92027E-06	0,117608
180	3,70255E-06	0,111076
190	3,50773E-06	0,105232
200	3,3324E-06	0,099972

0°

h см	E(h) CGSE	E(h) SI
0	0,028352072	850,5622
0,01	0,019892267	596,768
0,1	0,005397505	161,9251
1	0,000651351	19,54053
10	6,65103E-05	1,995308
20	3,32942E-05	0,998826
30	2,22048E-05	0,666145
40	1,66569E-05	0,499706
50	1,33271E-05	0,399812
60	1,11068E-05	0,333203
70	9,52061E-06	0,285618
80	8,33088E-06	0,249927
90	7,40547E-06	0,222164
100	6,6651E-06	0,199953
110	6,05931E-06	0,181779
120	5,55447E-06	0,166634
130	5,12728E-06	0,153818
140	4,76111E-06	0,142833
150	4,44375E-06	0,133312
160	4,16605E-06	0,124982
170	3,92103E-06	0,117631
180	3,70322E-06	0,111097
190	3,50834E-06	0,10525
200	3,33294E-06	0,099988

Hydrogen

80°

h, cm	E(h) CGSE	E(h) SI
0	0,00037436	11,23081
0,01	0,00037227	11,1681
0,1	0,000354456	10,63369
1	0,000239738	7,192135
10	5,65892E-05	1,697675
20	3,0608E-05	0,918239
30	2,0977E-05	0,62931
40	1,59563E-05	0,478689
50	1,28748E-05	0,386243
60	1,07908E-05	0,323725
70	9,28753E-06	0,278626
80	8,15187E-06	0,244556
90	7,26368E-06	0,21791
100	6,55002E-06	0,196501
110	5,96405E-06	0,178922
120	5,47432E-06	0,164229
130	5,05891E-06	0,151767
140	4,70209E-06	0,141063
150	4,3923E-06	0,131769
160	4,1208E-06	0,123624
170	3,88091E-06	0,116427
180	3,66742E-06	0,110023
190	3,47619E-06	0,104286
200	3,30392E-06	0,099117

0°

h см	E(h) CGSE	E(h) SI
0	0,000896571	26,89714
0,01	0,000884674	26,54021
0,1	0,000790289	23,70866
1	0,000382356	11,47069
10	6,20526E-05	1,861578
20	3,21385E-05	0,964154
30	2,16847E-05	0,650542
40	1,63625E-05	0,490875
50	1,3138E-05	0,394139
60	1,09751E-05	0,329253
70	9,42371E-06	0,282711
80	8,25659E-06	0,247698
90	7,34671E-06	0,220401
100	6,61746E-06	0,198524
110	6,01991E-06	0,180597
120	5,52134E-06	0,16564
130	5,09904E-06	0,152971
140	4,73675E-06	0,142102
150	4,42252E-06	0,132676
160	4,14739E-06	0,124422
170	3,90449E-06	0,117135
180	3,68847E-06	0,110654
190	3,49509E-06	0,104853
200	3,32099E-06	0,09963

Regolith

Plasma Waves over the Lunar Surface

The dusty plasma system over the lunar dayside contains photoelectrons, electrons and ions of the solar wind, neutrals, and fine dust particles. The photoelectron distribution function in the first approximation can be represented as a superposition of two Maxwellian distribution functions which are characterized by different electron temperatures and number densities. The first one is formed due to photons with energies in the vicinity of the work function of the lunar regolith while the second one is due to photons corresponding to the H Lyman-alpha line of the solar radiation spectrum. The relative motion of the solar wind with respect to the photoelectrons results in the excitation in a dusty plasma near the lunar surface of high-frequency oscillations with frequencies in the range of Langmuir and electromagnetic waves. The excitation of the dust acoustic waves is possible in the vicinity of the lunar terminator.

$$kv_{TiS} \ll kv_{Te1} \ll \omega \ll kv_{Te2} \ll kv_{TeS}$$

$$1 - \frac{\omega_{pe1}^2}{\omega^2} + \frac{1}{k^2\lambda_{De2}^2} - \frac{\omega_{piS}^2}{(\omega - ku_S)^2} = 0$$

$$\omega = ku_S\left(1 + i\omega_{piS}/\sqrt{\omega_{pe1}^2 - k^2u_S^2}\right)$$

$$k_{\max} \approx \omega_{pe1}/u_S \text{ and } \gamma_{\max} \approx \omega_{pe1}v_{Te2}/u_S$$

$$kv_{Td} \ll \omega \ll kv_{TiS}$$

$$1 + (1/k^2\lambda_{De1}^2) - (\omega_{pd}^2/\omega^2) = 0$$

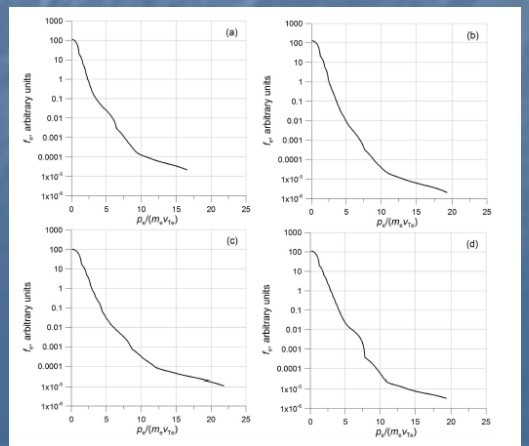

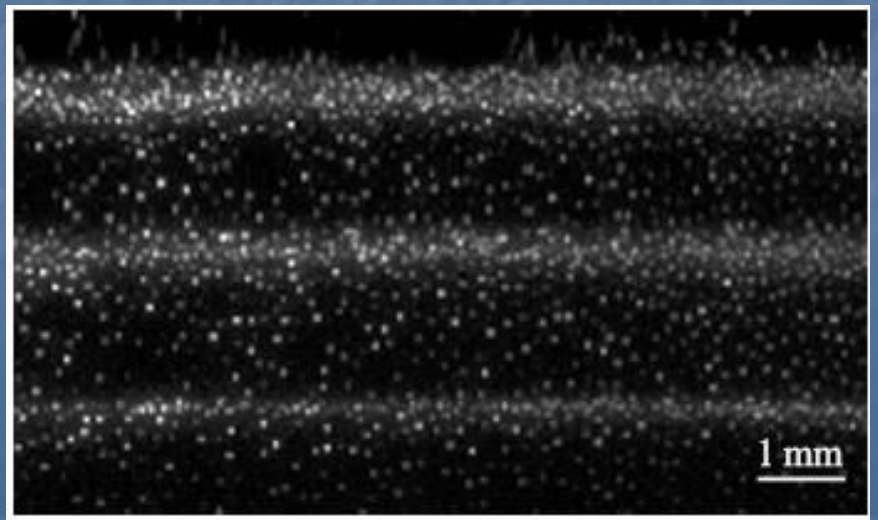

S. I. Popel, G. E. Morfill, P. K. Shukla, H. Thomas, J. Plasma Phys. **79**, 1071 (2013)

Electric Fields near the Terminator

$$\left(\frac{d\varphi}{d\xi}\right)^2 = 8\pi\left[n_{e0}T_e\left(\exp\left\{\frac{e\varphi}{T_e}\right\}-1\right)+n_{i0}T_i\left(\exp\left\{-\frac{e\varphi}{T_i}\right\}-1\right)+m_d u^2 n_{d0}\left(\sqrt{1+\frac{2eZ_d\varphi}{m_d u^2}}-1\right)\right]$$

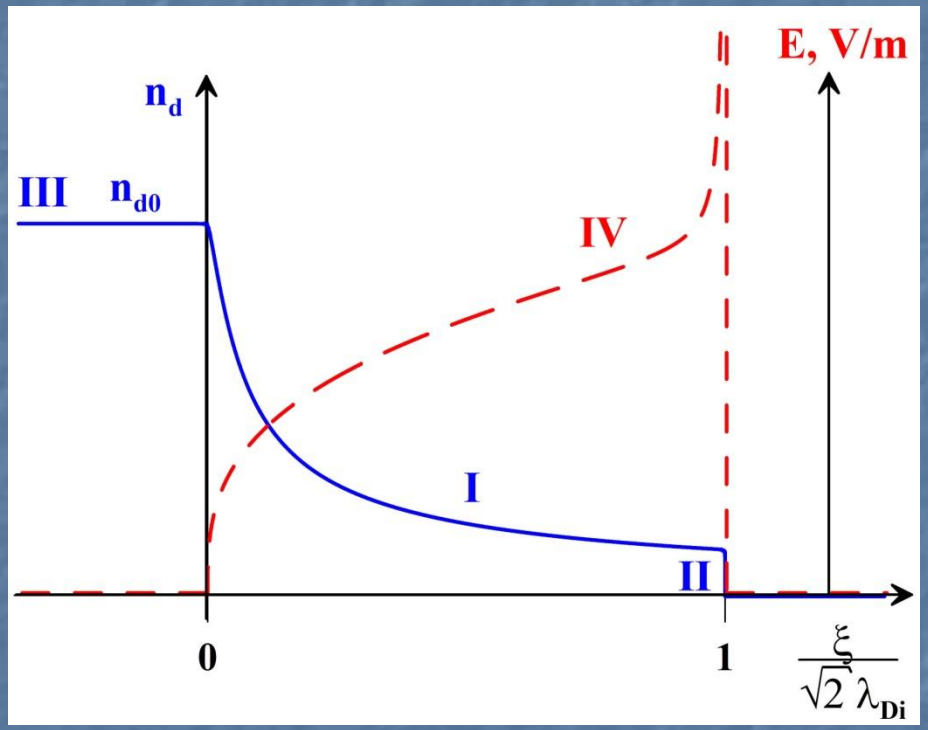

$$Z_d = -\frac{m_d}{e}u^2\frac{n_{d0}^2}{n_d^3}\frac{dn_d}{d\varphi}$$

$$u^2 \geq \frac{(n_{e0}-n_{i0})|Z_d|}{m_d\left(\frac{n_{e0}}{T_e}+\frac{n_{i0}}{T_i}\right)} \approx |Z_d|\frac{T_e}{m_d}$$

$$\varphi \to 0 \qquad \varphi \sim \varphi_0 \exp\left\{4\pi e^2\left[\frac{n_{e0}}{T_e}+\frac{n_{i0}}{T_i}-\frac{n_{d0}Z_d^2}{m_d u^2}\right]^{1/2}\xi\right\}$$

1) $\varphi_0 < 0$

$$I: \quad n_d = \frac{n_{d0}}{\sqrt{1+3\left(|Z_d|^2\frac{n_{d0}}{n_{i0}}\frac{\sqrt{3}T_i}{m_d u^2}\left(\frac{\xi}{\sqrt{2}\lambda_{Di}}\right)^2\right)^{2/3}}}$$

$$E = \sqrt{8\pi n_{i0}T_i}\left(\frac{|Z_d|}{3}\frac{n_{d0}^2}{n_{i0}^2}\frac{m_d u^2}{T_i}\frac{\xi}{\sqrt{2}\lambda_{Di}}\right)^{1/3}$$

$$II: \quad n_d = \frac{n_{d0}}{\sqrt{1-\frac{4T_i|Z_d|}{m_d u^2}\ln\left(1-\frac{\xi}{\sqrt{2}\lambda_{Di}}\right)}}$$

$$E = \frac{\sqrt{8\pi n_{i0}T_i}}{1-\xi/\sqrt{2}\lambda_{Di}}$$

$$E_{\max} = \sqrt{8\pi n_{i0}T_i}\exp\left\{\frac{m_d u^2}{4T_i|Z_d|}\left(\left(\frac{n_{d0}}{n_d^-}\right)^2-1\right)\right\}$$

Adhesion

- Apollo-17 astronaut Harrison Schmitt collects particles of lunar regolith. Lower part of his spacesuit is covered by dust.

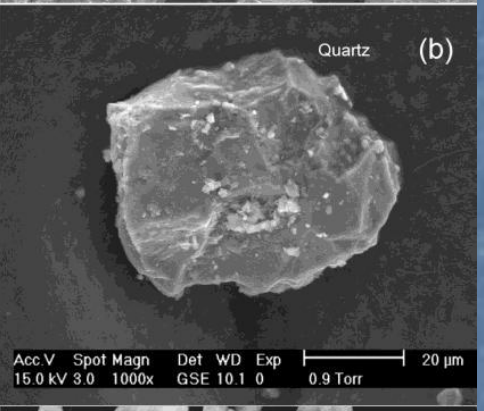

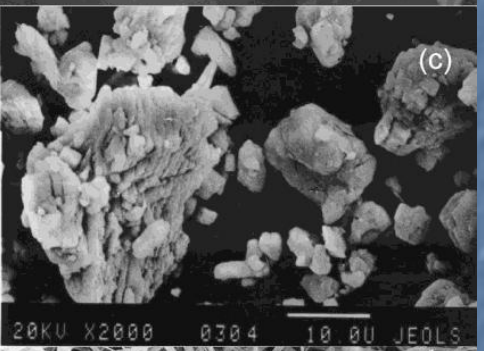

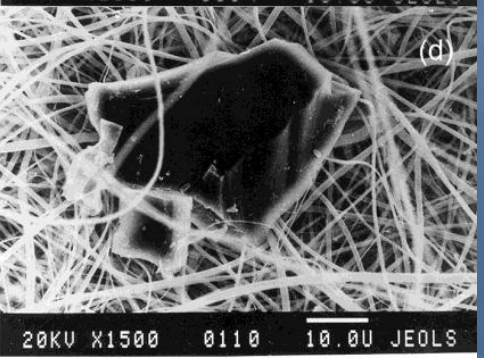

Adhesion

- To evaluate the adhesive force between two particles the following information is required: geometry of the particles, Hamaker's constant, as well as the properties of the surrounding media. Hamaker's constant characterizes the force which arises due to London–van der Waals attraction between two spheres and is estimated usually within the range of 10^{-21} J to 10^{-18} J depending on the chemical and mineral compositions. For lunar regolith Hamaker's constant is $4.3 \cdot 10^{-20}$ J. Rough particles of irregular form putted closely usually have a few points of contact. Without exact knowledge of number of contacts we provide calculation for one contact point. Two particles are modeled as smooth plane with half-spherical asperity and spherical particle of radius *a*. The final expression for the force of adhesion between a plane with an asperity of the radius r and a spherical particle is

$$F = \frac{AS^2}{24\Omega^2}\left(\frac{ra}{r+a} + \frac{a}{\left(1+rS/(2\Omega)\right)^2}\right)$$

Here, $S = \Omega/t$ is surface cleanliness. $\Omega = 0.132$ nm characterizes the diameter of oxygen ion while t determines the absorbed layer thickness. Surface cleanliness varies in the range of 1 to 0 and for lunar dayside is calculated as $S = 0.88$

Adhesion of rough particles of lunar regolith

Significant uncertainty exists as to the physical mechanism through which dust particles are released from the surface of the Moon. Adhesion has been identified as a significant force in the dust particle launching process which should be considered in future attempts to understand particle launching methods (Hartzell, C.M., Scheeres, D.J.: The role of cohesive forces in particle launching on the Moon and asteroids, Planet. Space Sci., Vol. 59, pp. 1758–1768, 2011).

The effect of roughness results in two-three orders of magnitude attenuation of the effect of adhesion. However, even considering the roughness of lunar regolith particles, the electrostatic forces required to launch dust particles from the lunar surface, as a rule, do not exceed the adhesive forces. Dust particle launching can be explained if the dust particles rise at a height of about dozens of nanometers owing to some processes. This is enough for the particles to acquire charges sufficient for the dominance of the electrostatic force over the gravitational and adhesive forces.

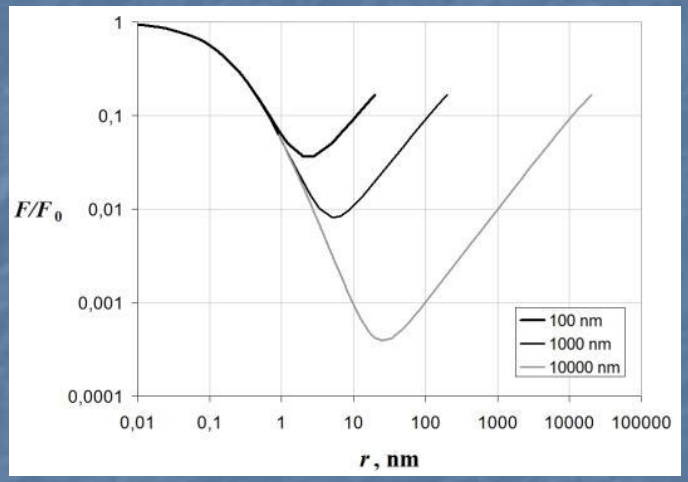

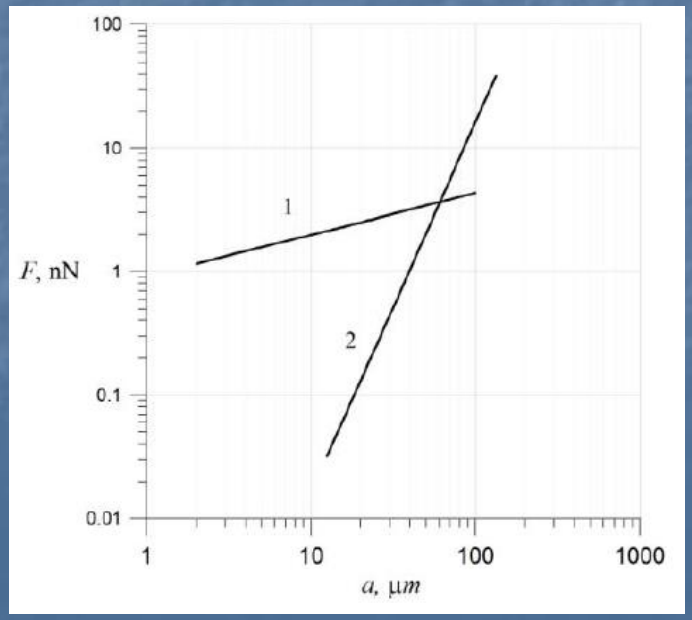

Release of dust particles from the lunar surface

- For each size of dust particles, there is a certain critical angle θ (larger than 74°) such that the rise of particles is impossible for angles θ smaller than this critical value. The reason for the indicated constraint is the fact that the condition of the separation of a positively charged dust particle from the positively charged surface of the Moon is the dominance of the electrostatic force over the attractive gravitational force. The electrostatic force depends on the charge of the particle, which in turn strongly depends on the density of photoelectrons. At θ values smaller than the critical value, photoelectrons that are incident on the dust particle and reduce its (positive) charge prevent the dominance of the electrostatic force over the attractive gravitational force. However, owing to the sharp decrease in the density of photoelectrons with an increase in the height, even at angles θ smaller than the critical value, the dust particle rising at a height of about 1 mm owing to some processes: heating by solar radiation and cooling as well as inhomogeneities of the surface of the Moon.

Effects of Micrometeoroids (I)

- When high-speed meteoroid impacts the lunar surface the substances of the impactor and the target are strongly compressed and heated. Under the action of high pressure strong shock wave is formed. The shock propagates and weakens moving away from the impact epicenter. Finally the weakening shock transforms into linear acoustic wave. The zones (around the impact epicenter) of evaporation of the substance, its melting, destruction of particles constituting lunar regolith, their irreversible deformations are formed due to the propagation of the weakening wave. Beyond the zone of irreversible deformations the zone of elastic deformation is created which is characterized by the magnitudes of the pressure in acoustic wave less than dynamic limit of elasticity.

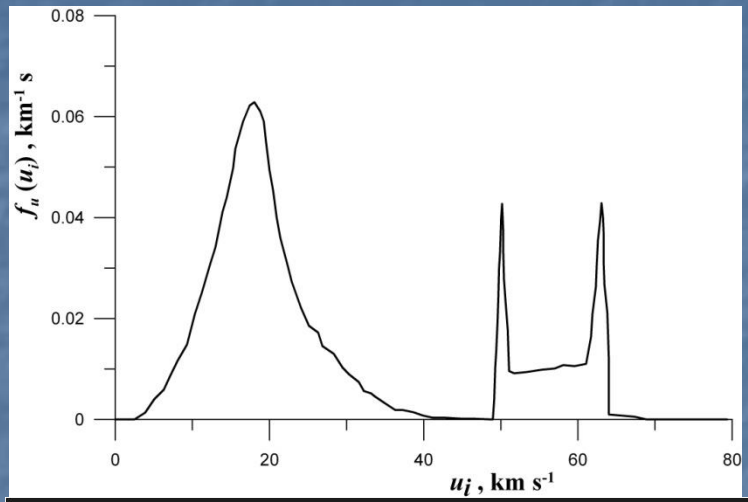

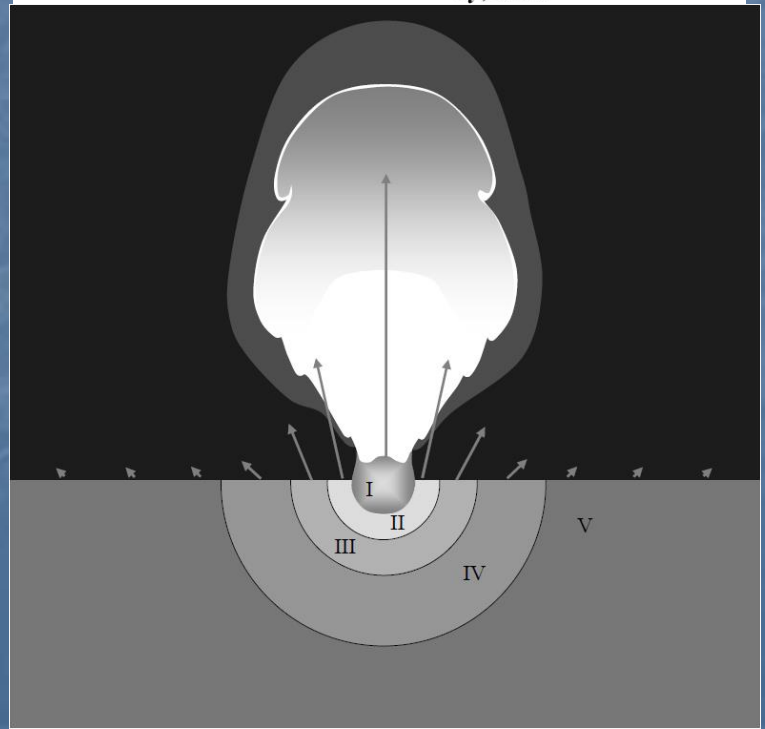

Effects of Micrometeoroids (II)

- Considering the balance between the maximum force of pressure in the blast wave and the sum of the adhesive, electrostatic, and gravitational forces we determine the radius of the zone around the impact epicenter which restricts the region where dust particles are released from the surface of the Moon due to meteoroid impacts. Furthermore, we estimate the speeds of the released particles, find their size-distribution, and evaluate maximum heights of dust particle rise.

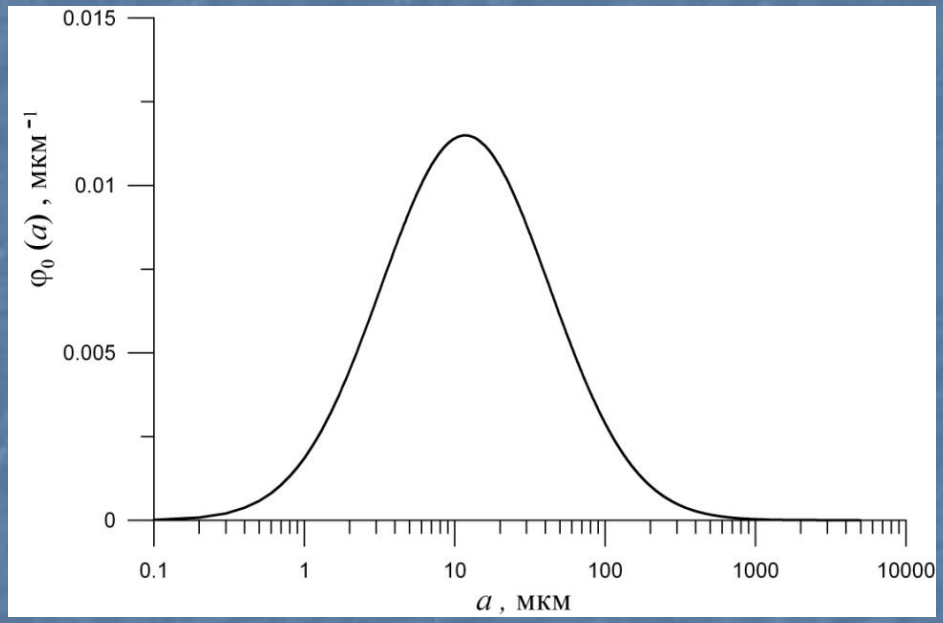

h=0.1 m N=65 m^{-2} (24 hours)^{-1}

h=1 m N=20 m^{-2} (24 hours)^{-1}

h=10 m N=7 m^{-2} (24 hours)^{-1}

Dust at high altitudes

- Dusty plasma effects do not result in the rise of 100 nm dust particles up to the altitudes of about 100 km over the lunar surface. To explain the presence of 100 nm grains at altitudes of about 100 km the so-called dynamic fountain model for lunar dust has been proposed. But the dynamic fountain model for lunar dust is one of many ways in which dust could interfere with science and exploration activities on the Moon.
- Another phenomenon which can be responsible for an appearance of dust particles at the altitudes of about 100 km is related to impacts of meteoroids or man-made projectiles with the surface of the Moon.

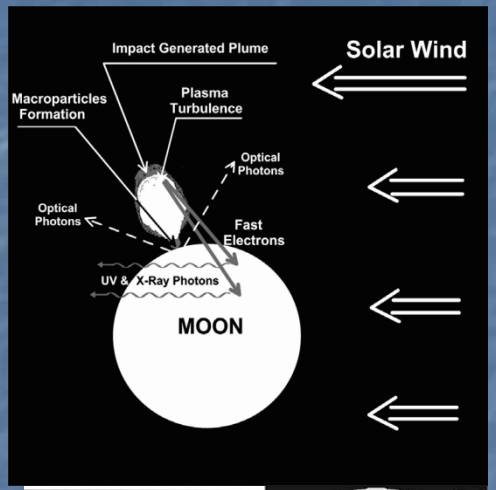

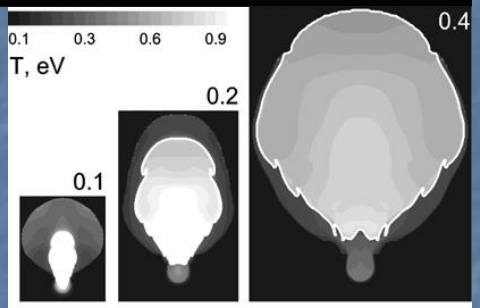

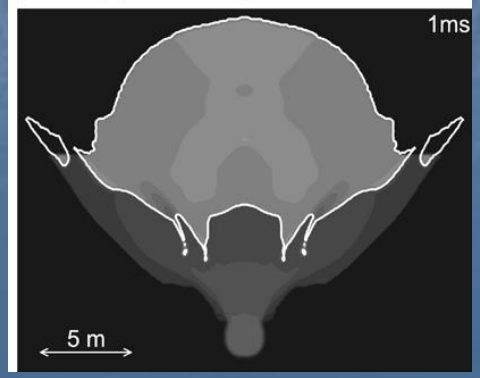

Phobos and Deimos

Mars's two potato-shaped worlds are tiny – Phobos is the dimensions of 27 × 22 × 18 km and Deimos is highly non-spherical with triaxial dimensions of 15 × 12.2 × 11 km, making it 0.56 times the size of Phobos. So their gravitational pull is only one-thousandth that of Earth, making landing on them more like docking with a spaceship. That translates to big savings for a crewed mission to the moons compared with one to the Martian surface. For now, the only planned missions to the moons are robotic. Russia is gearing up to launch the Phobos-Grunt II missionin 20?? that will attempt to land a craft on Phobos, collect the first samples from the moon's surface and return them to Earth. The project could help determine if there is any hydrogen or water present, which astronauts on a later crewed mission could use. If Phobos-Grunt II is successful, then NASA send a robotic mission to Deimos, about which even less is known than its larger cousin.

Dusty plasmas at Phobos and Deimos

A weak gravitational field enhances the role of dust on Phobos and Deimos because even a weak perturbation can result in the formation of a massive dust cloud over the surface of this Martian satellite. Among the aims of the Phobos-Grunt 2 mission are to detect dust particles in an orbit around Mars and near the surface of Phobos and to determine the main parameters of dust particles (momentum, mass, velocity, and charge). Furthermore, the measurement of the plasma parameters and the determination of the local electric field near the surface of Phobos are expected. To these ends, piezoelectric impact sensors, whose operation is based on the impact action of a dust particle (see bottom Fig.), and probes for measurements of the parameters of the plasma and the local electric field near the surface of Phobos will be used.

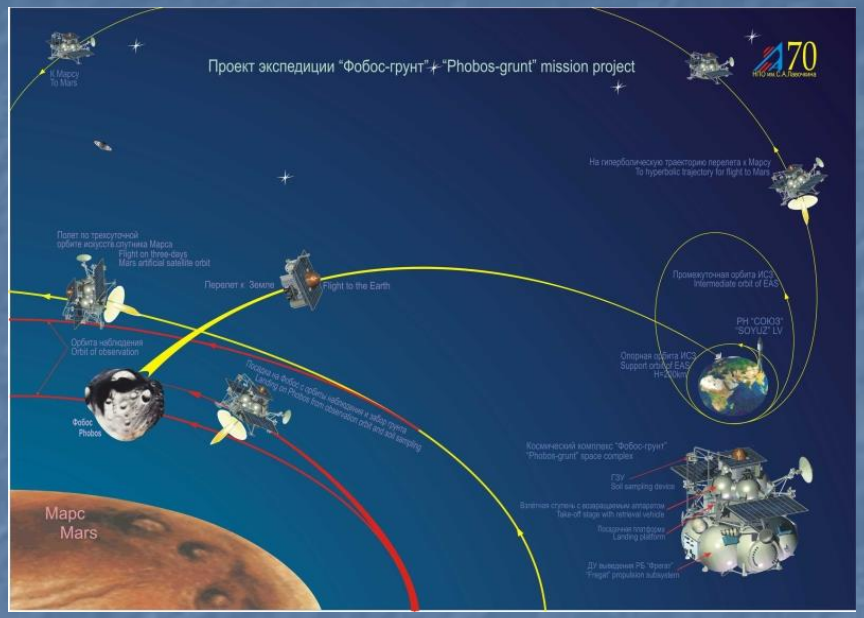

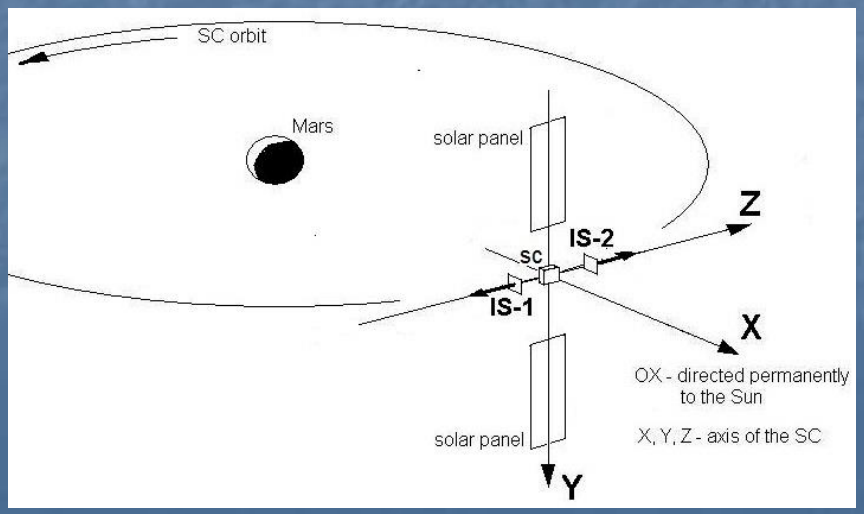

Solar spectra at Phobos and Deimos

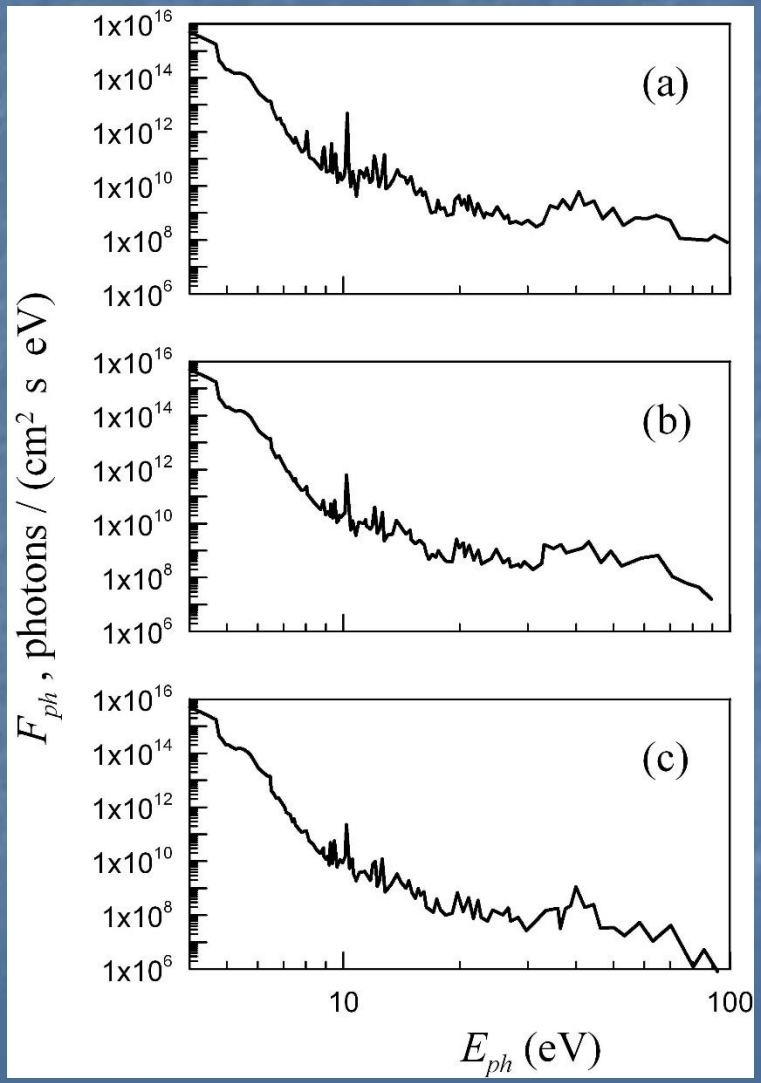

The shape of spectra of solar radiation corresponds to the shape of spectra near the Moon, but the intensity is lower because the solar constant in the orbit of Mars is 592 W/m^2, which is 43% of the solar constant in the orbit of the Earth. Correspondingly, spectra of solar radiation in the orbit of Mars vary significantly during an 11-year cycle of solar activity. However, despite the variation of the energy emitted by the Sun in the ultraviolet range (primarily, from the point of view of emission of photoelectrons) in the indicated cycle, significant (by orders of magnitude) variations of number density of photoelectrons and values of their temperature do not occur.

Photoelectron distributions at Phobos and Deimos

(Solid lines) Energy distribution functions of photoelectrons near the illuminated part of the surface of Phobos corresponding to the (a) X28 solar flare, (b) solar maximum, and (c) solar minimum. The work function is W = (squares) 6 and (triangles) 5.5 eV. The dashed lines are the Maxwellian distributions that are calculated for average energies of photoelectrons characterizing the corresponding distributions shown by solid lines and almost coincide at W = 6 and 5.5 eV.

Table 1. Parameters of photoelectrons in the surface layer of the illuminated part of Phobos for various solar activity levels (I, II, III) and various work functions (see the main text)

Parameter	I	II	III
N_{01} (cm^{-3})	3.7×10^1	1.3×10^1	0.57×10^1
T_{e1} (eV)	2.1	1.9	1.2
N_{02} (cm^{-3})	3.7×10^1	3.7×10^1	0.65×10^1
T_{e2} (eV)	2.1	1.9	1.2

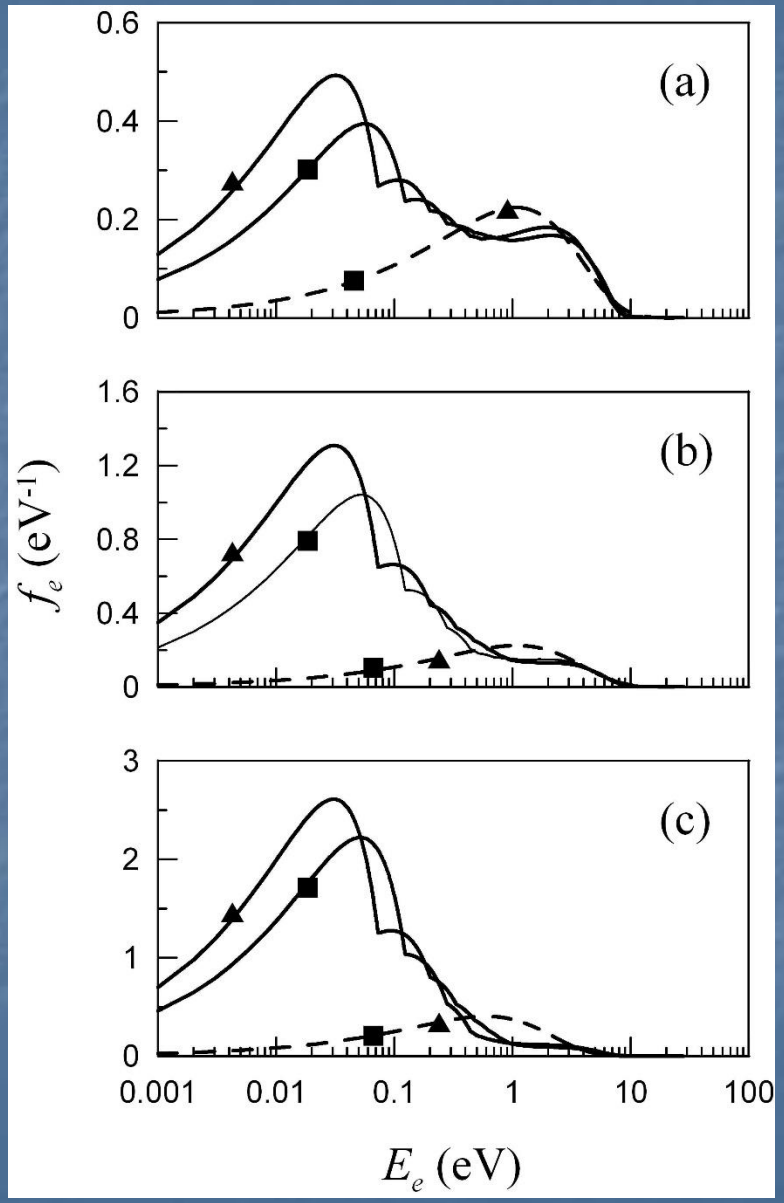

Dust distributions at Phobos and Deimos

Photoelectric and electrostatic processes in the near-surface layer over the illuminated part of Phobos and Deimos result in the formation of the dusty plasma for subsolar angles exceeding about 76°. Within the physicomathematical model for the self-consistent description of densities of photoelectrons and dust particles over the surface of the illuminated part of Phobos and Deimos, we obtained the altitude dependences of the density of dust particles, their charges and sizes, and electric fields. It has been shown that dust particles with the characteristic sizes of about μm rise over the surfaces of Phobos and Deimos and electric fields with a strength of about 1 V/m exist near their surfaces. The typical densities of dust particles and photoelectrons are ~ 0.01 – 0.1 cm^{-3} and 10 cm^{-3}, respectively.

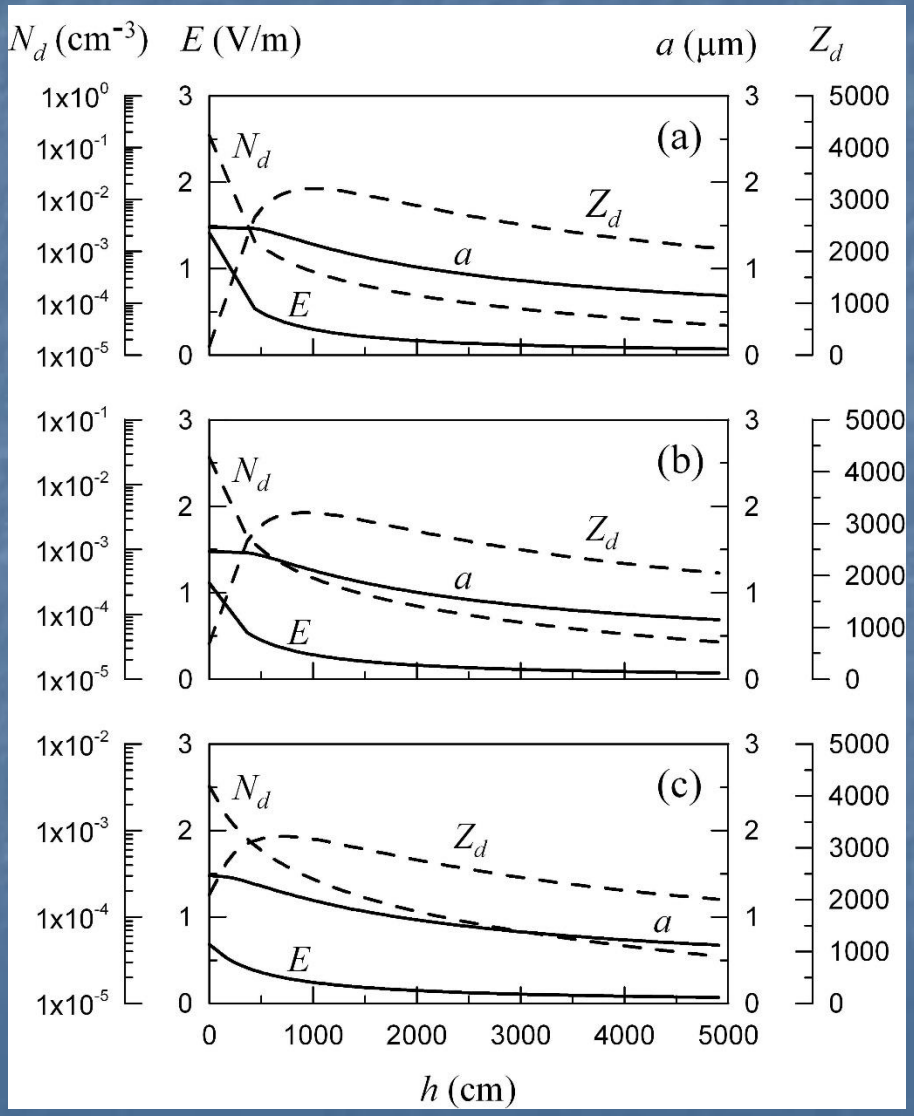

Comets

Calculations are performed for the parameters of Halley's comet. It nucleus has the potato-shaped form, $M = 2.2 \cdot 10^{14}$ kg, $\varrho = 600$ kg/m^3, the dimensions are 15 × 8 × 8 km. Astrophysics escape velocity is 2.57 m/s.

Typical speed of dusts over the surface is ~ 1 m/s at h ~ 1 m, and ~ 10 m/s at h ~ 1 km.

Thus we can expect dust particle fluxes from the surface of the comet due to the electrostatic effects ~ 100 particles $m^{-2} \cdot s^{-1}$.

The problem should be solved with taking into account the evaporation processes from the surface of the nucleus (the speed of the gas beyond the front of the evaporation wave is 330 m/s).

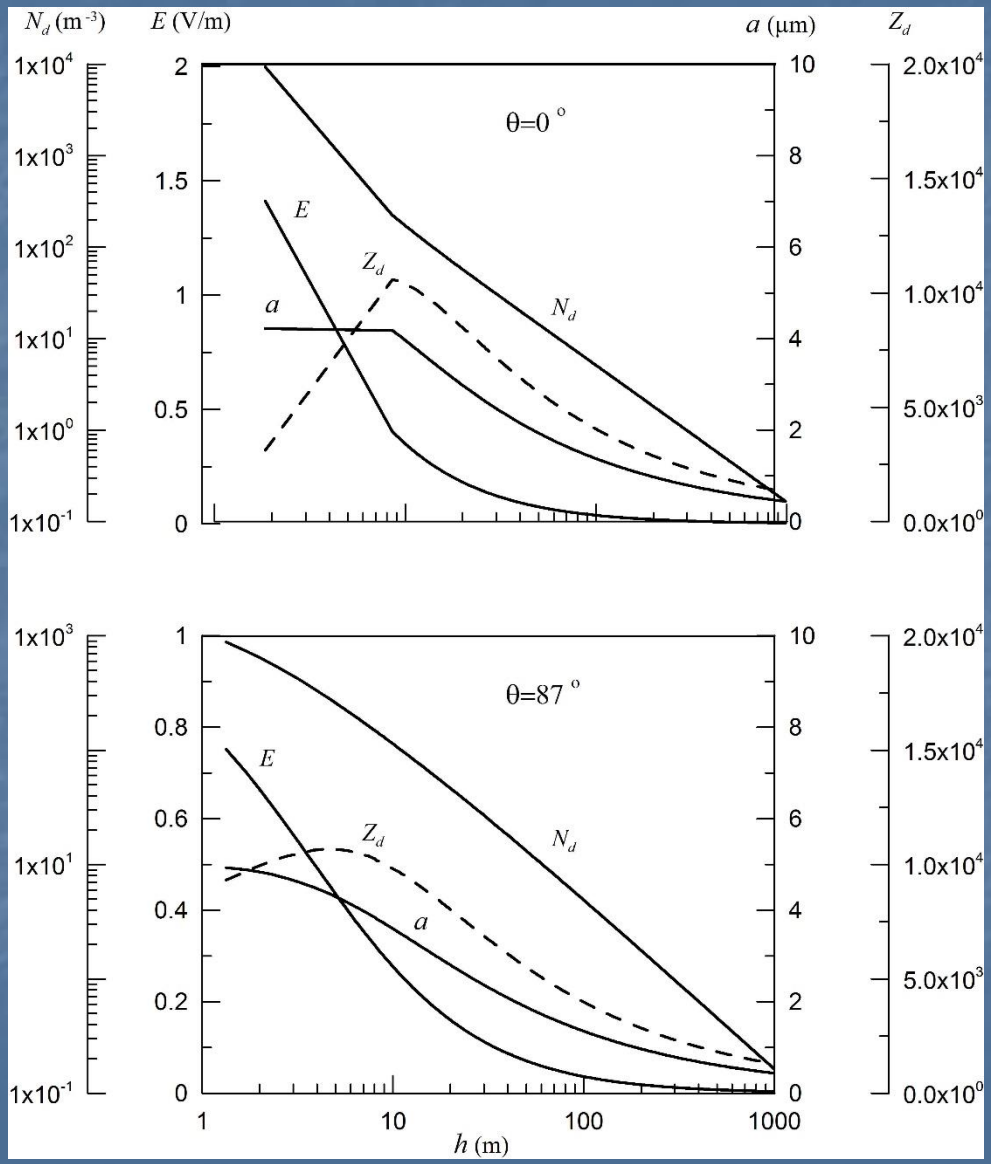

Interaction of Solar wind with comet (I)

- Solar Wind interacts with the dust of comets.
- Cometary comae contain dust grains with n up to 10^{11} cm^{-3} . The characteristic size of the coma is 10^6 km.
- Cometary tails are ~ 10^7 km in length and ~ 10^5 km in diameter. The dust density is n ~ 10^{-3} – 10^{-7} cm^{-3}. A size distribution is n(a) ~ a•10^{-s} (s still uncertain).
- Main composition of interplanetary and cometary dust:

  60% chondritic (Fe, Mg, Si, C, S)

  30% iron-sulphur-nickel

  10% silicates (olivine)

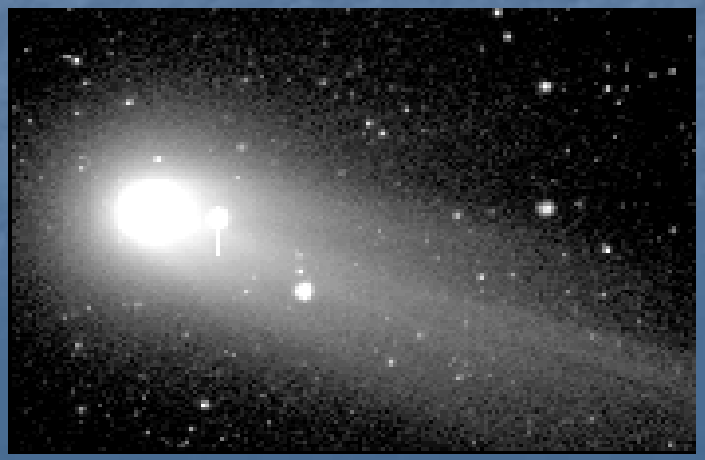

Interaction of Solar wind with comet (II)

- The presence of dust in cometary coma can modify shock wave formed as a result of Solar Wind interaction with a comet.
- The outer shock wave (bow shock) can be considered as an ion-acoustic shock wave, because it is formed as a result of the interaction of cometary ions with protons of Solar Wind => its modification by dust particle charging process.
- Possible formation of dust structures in the region of the interaction of Solar Wind with cometary coma.

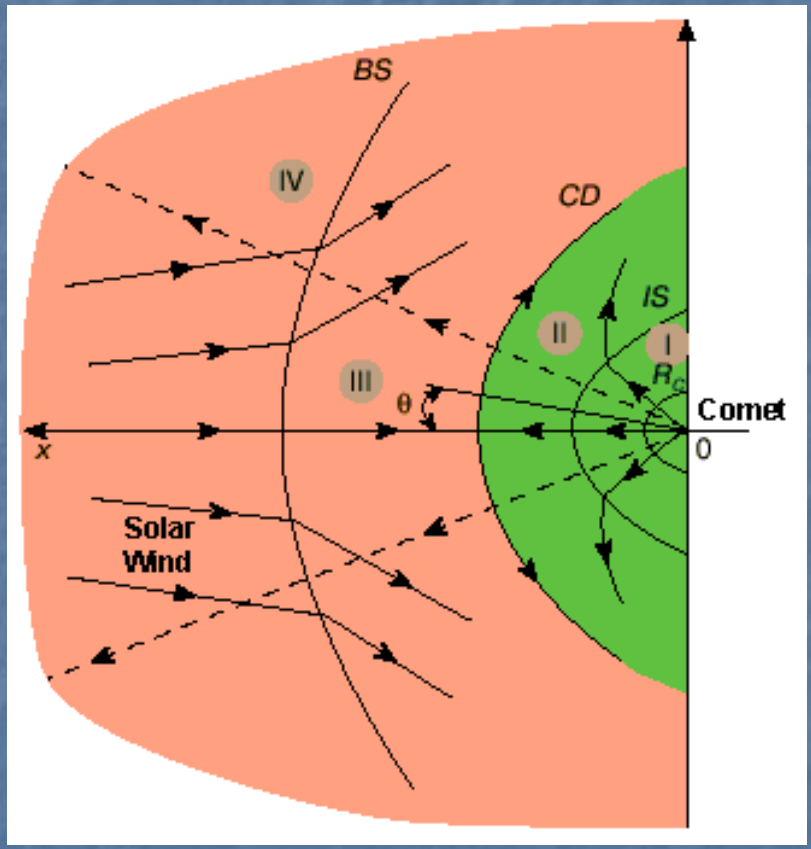

Model

- The **self-consistent model** takes into account solar radiation, dust particle charging, evaporation and formation of neutral particles, photoionization, electric fields; the evolution of Solar Wind ions and cometary ions, of dust particles as well as of the dust charge variation.

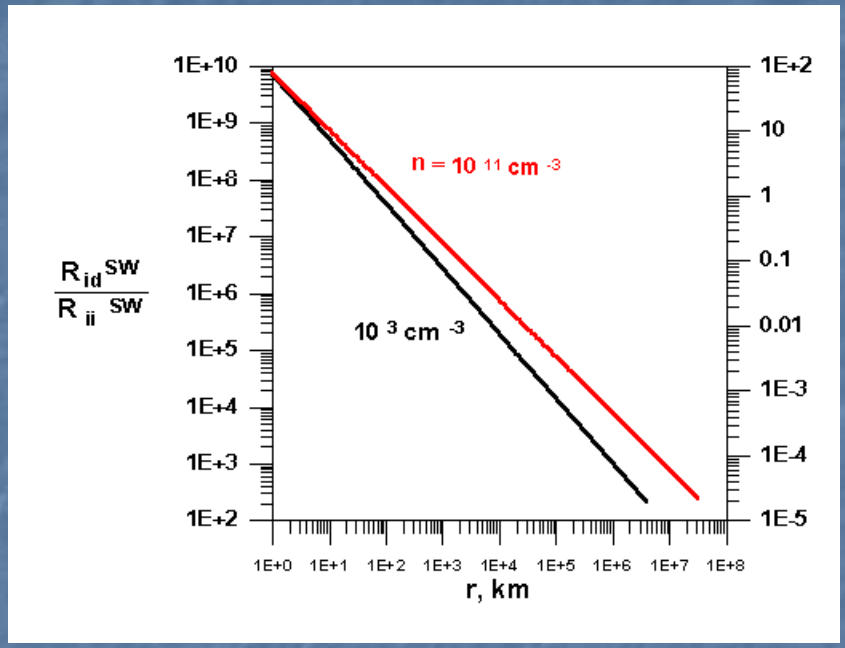

$$m_p n_p \frac{dV_{p\alpha}}{dt} = -\frac{\partial p_p}{\partial x_\alpha} + \eta^{SW} \frac{\partial W_{p\alpha\beta}}{\partial x_\beta} - e n_p \frac{\partial \varphi}{\partial x_\alpha} + R_{id}^{SW} + R_{ii}^{SW}, \qquad W_{p\alpha\beta} = \frac{\partial V_{p\alpha}}{\partial x_\beta} + \frac{\partial V_{p\beta}}{\partial x_\alpha} - \frac{2}{3}\delta_{\alpha\beta}\mathrm{div}\mathbf{V}$$

Conclusions

- Dusty plasmas exists at different atmosphereless cosmic bodies (the Moon, Phobos and Deimos, comets, etc.). The future experimental investigations assume investigations of dust and dusty plasmas on the Moon (Luna-Glob and Luna-Resource) as well as on Phobos (Phobos-Grunt-2). Models of dusty plasma systems over the Moon, Phobos, Deimos, and comets are developed and it is shown that the dusty plasma systems include charged dust, photoelectrons, and electrons and ions of the solar wind. The problem of dusty plasmas at the comets is interesting from the viewpoint of the description of dusty coma formation. We discuss also the interaction of the solar wind with dusty cometary comae resulting in the formation of bow shock with the structure determined by the process of anomalous dissipation in dusty plasmas related to dust particle charging.